AFOSR-TR- 88-1274

D SPECTRUM MOBILE RADIO COMMUNICATIO

under contract

AFOSR-82-0309

with

Air Force Office of Scientific Research
Bolling Air Force Base
Washington, D.C.

Electrical Engineering Department

School of Engineering and Applied Science

Southern Methodist University

Dallas, Texas 75275

(2)

SPREAD SPECTRUM MOBILE RADIO COMMUNICATIONS

under contract

AFOSR-82-0309

with

Air Force Office of Scientific Research
Bolling Air Force Base
Washington, D.C.

INTERIM SCIENTIFIC REPORT

October 1, 1987 -

September 30, 1988

S.C. GUPTA, PRINCIPAL INVESTIGATOR

Electrical Engineering Department

School of Engineering and Applied Science

Southern Methodist University

Dallas, Texas 75275

SECURITY CLASSIFICATION OF THIS PAGE

REPORT DOCUMENTATION PAGE

1a. REPORT SECURITY CLASSIFICATION UNCLASSIFIED	1b. RESTRICTIVE MARKINGS
2a. SECURITY CLASSIFICATION AUTHORITY	3. DISTRIBUTION/AVAILABILITY OF REPORT: Approved for public release; distribution unlimited.
2b. DECLASSIFICATION/DOWNGRADING SCHEDULE	
4. PERFORMING ORGANIZATION REPORT NUMBER(S)	5. MONITORING ORGANIZATION REPORT NUMBER(S): AFOSR-TR- 88-1274
6a. NAME OF PERFORMING ORGANIZATION: Electrical Engineering Dept. Southern Methodist University; 6b. OFFICE SYMBOL (If applicable)	7a. NAME OF MONITORING ORGANIZATION: AFOSR
6c. ADDRESS (City, State and ZIP Code): Dallas, Texas 75275	7b. ADDRESS (City, State and ZIP Code): Bldg 410 Bolling AFB, DC. 20332
8a. NAME OF FUNDING/SPONSORING ORGANIZATION: AFOSR/NE; 8b. OFFICE SYMBOL (If applicable): NE	9. PROCUREMENT INSTRUMENT IDENTIFICATION NUMBER: AFOSR-82-0309
8c. ADDRESS (City, State and ZIP Code): Building 410, Bollings AFB Washington D.C. 20332-6448	10. SOURCE OF FUNDING NOS.

PROGRAM ELEMENT NO.	PROJECT NO.	TASK NO.	WORK UNIT NO.
61102F	2305	B3	

11. TITLE (Include Security Classification): Spread Spectrum Mobile Radio Communication

12. PERSONAL AUTHOR(S): S.C. Gupta, C. Sandeep, W. Refai

13a. TYPE OF REPORT	13b. TIME COVERED	14. DATE OF REPORT (Yr., Mo., Day)	15. PAGE COUNT
	FROM 10/1/87 TO 9/30/88	1988, October 30	67

16. SUPPLEMENTARY NOTATION

17. COSATI CODES		
FIELD	GROUP	SUB. GR.

18. SUBJECT TERMS (Continue on reverse if necessary and identify by block number): Bandwidth Efficient Modulation, Multipath Diversity Receivers, PRCPM Schemes, Indoor Wireless Communication Receivers

19. ABSTRACT (Continue on reverse if necessary and identify by block number)

In this report two problems are studied. The first is concerned with evaluating the performance of a class of bandwidth efficient modulation schemes in a frequency reuse mobile radio channel. This work is presented in Chapter 1 and 2. The second problem is concerned with formulating and evaluating the performance of a class of known delay multipath diversity receivers for indoor wireless communication. This work is presented in chapter 3 and 4.

In chapter 1 several Partial Response (PRCPM) schemes such as TFM, GMSK and 3RC are compared with regard to their performance in the presence of Adjancent Channel Interference (ACI) and Cochannel Interference (CCI). The performance criteria chosen were average probability of bit error and mean-square crosstalk ratio. A comparison of three receiver filters with regard to their ability to reject ACI is also provided. Results indicate that receiver filter length is a very important parameter for good performance.

(see back of page)

20. DISTRIBUTION/AVAILABILITY OF ABSTRACT: UNCLASSIFIED/UNLIMITED ☒ SAME AS RPT. ☐ DTIC USERS ☐	21. ABSTRACT SECURITY CLASSIFICATION: UNCLASSIFIED
22a. NAME OF RESPONSIBLE INDIVIDUAL: ~~S.C. Gupta~~ Gibbs	22b. TELEPHONE NUMBER (Include Area Code): ~~(214) 692-3113~~ (202) 767-4931; 22c. OFFICE SYMBOL: NE

DD FORM 1473, 83 APR EDITION OF 1 JAN 73 IS OBSOLETE.

SECURITY CLASSIFICATION OF THIS PAGE

19. continued:

In chapter 2 the performance of PRCPM schemes is analyzed by considering the combined effects of ACI, CCI and Rayleigh fading. The analysis is extended to the case when space diversity is employed. Results indicate that by using space diversity and Maximal Ratio Combining significant performance gains can be achieved.

Indoor wireless communication receivers must contend with a severe multipath problem. By using Direct Sequence Spread Spectrum (DSSS) signaling multipath diversity receivers can be used to mitigate the effects of frequency selective fading. In chapter 3 a class of such adaptive multipath diversity receivers are developed and their performance evaluated for uniform and non-uniform delay power profiles. The performance evaluation considers the effects of delay power profile shape, RMS delay spread, signaling alphabet size, diversity order and source modulation.

In chapter 4 the three receivers derived in Chapter 3 are compared with regard to their performance in an illustrative asynchronous CDMA system. The intended application is for indoor wireless communication network. Theoretical performance analysis is presented based on a set of simplifying assumptions. These assumptions are later justified through a simulation study.

Summary

In this report, two problems are studied. The first is concerned with evaluating the performance of a class of bandwidth efficient modulation schemes in a frequency reuse mobile radio channel. This work is presented in chapter 1 and 2. The second problem is concerned with formulating and evaluating the performance of a class of known delay multipath diversity receivers for indoor wireless communication. This work is presented in chapter 3 and 4.

In chapter 1, several partial response (PRCPM) schemes such as TFM, GMSK and 3RC are compared with regard to their performance in the presence of Adjacent Channel Interference (ACI) and CoChannel Interference (CCI). The performance criteria chosen were average probability of bit error and mean-square cross talk ratio. A comparison of three receiver filters with regard to their ability to reject ACI is also provided. Results indicate that receiver filter length is very important parameter for good performance.

In chapter 2, the performance of PRCPM schemes is analyzed by considering the combined effects of ACI, CCI and Rayleigh fading. The analysis is extended to the case when space diversity is employed. Results indicate that by using space diversity and Maximal Ratio Combining significant performance gains can be achieved.

Indoor wireless communication receivers must contend with a severe multipath problem. By using Direct Sequence Spread Spectrum (DSSS) signaling multipath diversity receivers can be used to mitigate the effects of frequency selective fading. In chapter 3, a class of such adaptive multipath diversity receivers are developed and their performance evaluated for uniform and non-uniform delay power profiles. The performance evaluation considers the effects of delay power profile shape, RMS delay spread, signaling alphabet size, diversity order and source modulation.

In chapter 4, the three receivers derived in chapter 3 are compared with regard to their performance in an illustrative asynchronous CDMA system. The intended application is for indoor wireless communication network. Theoretical performance analysis is presented based on a set of simplifying assumptions. These assumptions are later justified through a simulation study.

Table of Contents

CHAPTER 1

PERFORMANCE COMPARISON OF PRCPM SCHEMES WITH INTERFERING SIGNALS

1.1 Introduction

Partial Response Continuous Phase Modulation (PRCPM) schemes have recently attracted attention because of their improved performance capabilities over traditionally used digital modulation schemes. These capabilities occur from observing the signal over more than one symbol interval, thereby utilizing the memory inherent in the continuous phase transitions.

The ultimate measure in a digital communication system is the probability of error. However, formulation in terms of the error probability is feasible only in simple cases. Often an intermediate measure is required to be considered and the error probability has to be evaluated under certain simplifying assumptions. In the adjacent channel interference problem the intermediate measures usually considered are the mean-square crosstalk and the worst-case crosstalk [1,7]. The worst-case crosstalk and usually requires extensive simulation to compute, while mean-square crosstalk is much more amenable to mathematical formulation and also has the meaning of noise variance.

This chapter presents the signal to mean-square crosstalk as a performance measure among a selected set of receiver filters for various CPM schemes. Also, it simulates and compares the error performance in the presence of ACI (with a different number of interferers) for various CPM schemes and among the AOF receiver with observation intervals of three and four bits. In the next section we will introduce the various modulation schemes that have been used throughout our work and emphasize an easy way to calculate the power spectra.

1.2 Modulation Schemes

The bandwidth efficiency of a modulation scheme is defined as the ratio of the bit rate transmitted to the bandwidth used. This is equivalent to the number of transmitted bits per cycle of channel bandwidth. We have shown in Equation 1.1 and have repeated here for convenience

$$\text{Bandwidth Efficiency} = \frac{\log_2 M}{BT}, \qquad \text{bits/sec/Hz} \tag{1.1}$$

that signals with small BT products are the most bandwidth efficient,

while no single universal definition is available for bandwidth. Amoroso [15] has shown that power spectral density is a key parameter in the definition of bandwidth efficiency. We will use this approach to evaluate numerically the spectrum of various modulation schemes as a measure of the bandwidth efficiency.

The modulation schemes and the corresponding pulse shapes considered in this work are Raised Cosine (RC)

$$g(t) = \begin{cases} \frac{1}{2LT}\left(1 - \cos\left(\frac{2\pi t}{LT}\right)\right) ; & o \leq t \leq LT \\ o ; & \text{otherwise} \end{cases} \tag{1.2}$$

The frequency pulse g(t) is a raised cosine over L symbol intervals and the scheme is defined as LRC.

Tamed Frequency Modulation (TFM)

$$g(t) = \frac{1}{8}\left[g_o(t-T) + 2g_o(t) + g_o(t+T)\right] \tag{1.3}$$

where

$$g_o(t) \simeq \frac{1}{T}\left[\frac{\sin\left(\frac{\pi t}{T}\right)}{\left(\frac{\pi t}{T}\right)} - \frac{\pi^2}{24}\right] \left[\cdot \frac{2\sin\left(\frac{\pi t}{T}\right) - 2\left(\frac{\pi t}{T}\right)\cos\left(\frac{\pi t}{T}\right) - \left(\frac{\pi t}{T}\right)^2 \sin\left(\frac{\pi t}{T}\right)}{\left(\frac{\pi t}{T}\right)^3}\right] \tag{1.4}$$

Gaussian MSK (GMSK)

$$g(t) = \frac{1}{2T}\left[Q\left[2\pi B_b \frac{t - \frac{T}{2}}{\sqrt{\ln 2}}\right] - Q\left[2\pi B_b \frac{t + \frac{T}{2}}{\sqrt{\ln 2}}\right]\right] \tag{1.5}$$

where Q(x) is the Gaussian error function.

1.3 Error Probability Measure in Interfering Environment

The desired transmitted signal is given by:

$$S(t, \underline{\alpha}) = \sqrt{\frac{2E}{T}} \cos(\omega_c t + \phi(t, \underline{\alpha})) \tag{1.6}$$

where $\underline{\alpha} = \alpha_0, \cdots \alpha_{n-1}, \alpha_n, \cdots$ is an infinitely long sequence of independent binary data symbols, taking values ± 1. E is the symbol energy and T is the symbol time. f_o is the carrier frequency and the information carrying phase is given by:

$$\phi(t, \underline{\alpha}) = 2\pi h \sum_{i=-\infty}^{\infty} \alpha_i \, q(t - iT) \tag{1.7}$$

h is the modulation index. The phase response q(t) is defined by:

$$q(t) = \int_{-\infty}^{t} g(\tau) \, d\tau$$

where $g(\tau)$ is the frequency pulse function.
The adjacent channels are distributed two on each side of the desired channel. Due to the symmetry between both sides, one side is introduced and the other is similar.

The interfering signals on one side of the desired channel are $\sum_{k=1}^{2} s_I(t,\beta_k)$ for $1 \leq k \leq 2$. ν_k for $1 \leq k \leq 2$ are the amplitude of the interfering signals and are assumed to be unity among the k interferers. The center frequency of the first interferer ω_1 is $\Delta\omega$ rad/sec away from ω_o and the second interferer $\omega_2 = 2\omega_1$ is $2\Delta\omega$ red/sec away from ω_o. There is a delay of τ and 2τ secs between the first and second interfering signals and $s(t,\underline{\alpha})$ respectively. Also ς_k for $1 \leq k \leq 2$ are the random phase offests. This implies that the interfering signals are independent of one another and of the desired signal. The interfering signals can be represented as

$$\sum_{k=1}^{2} s_I(t,\beta_k) = \nu \sqrt{\frac{2E}{T}} \sum_{k=1}^{2} \cos\left[\omega_k(t-\tau_k) + \psi(t-\tau_k,\beta_k) + \varsigma_k\right] \tag{1.8}$$

τ_k and ς_k are uniformly distributed in the range [0, T] and $[0, 2\pi]$ respectively. The simulated probability of error for the whole model is given by

$$(P^*_{\theta} / s^-_j) = \frac{1}{N_s} \sum_{i=1}^{N_s} \left[\frac{1}{16} \sum_k \sum_l \sum_m \sum_n P\,(\eta > x_j + k\, x_{I1_i})\right]$$

$$\left[\frac{1}{1}(+l\,x_{I2_i}+m\,x_{I3_i}+n\,x_{I4_i})\right]\cdot W_i \qquad (1.9)$$

where k, l, m, and n take values ± 1 with equal probability. x_{Ik} for $1 \leq k \leq 4$ are the outputs due to the interfering signals and are computed numerically. W_i is the weight of the pdf of the noise and is used to reduce the computational time (Modified Monte-Carlo method).

The error performance of various schemes has been investigated with and without the effect of ACI over an AOF receiver with observation length of 3 bits. Figure 1.1 shows the theoretical probability of error and it shows that the MSK scheme performs better than 3RC or TFM5 or GMSK5. The excellent correlation between the theoretical results and the simulated results in the absence of ACI is shown in the same figure. This gives us confidence about the accuracy of the estimates.

The simulated error probability with the effect of ACI at different channel spacings (Δf) is illustrated in Figure 1.2 and 1.3 for Δf=0.8 and 1.2 respectively. It can be seen in Figure 1.2 that MSK and GMSK5 with βT=0.2 are severely degraded at Δf=0.8 till the point that error probability of 10^{-5} was unattainable at SNR=14 dB, while 3RC and TFM5 schemes both have a better ACI rejection at the same channel spacing. At larger channel spacing (Δf=1.2) shown in Figure 1.3, MSK has the best error performance due to less effect of ACI at larger channel spacing, 3RC and TFM5 both have better ACI rejection, but GMSK5 still degrades badly and error probability of 10^{-5} was unattainable at SNR=12 dB.

In Figure 1.4, we looked at the theoretical error probability for CPM schemes at a larger receiver observation length (four bits). Both TFM and GMSK schemes with (βT=0.25) were truncated over four bit periods. It was found that for AOF(4T), GMSK4 outperforms TFM4 while the 3RC scheme performs the best among all of them. The error probability with two interferers (k=2) at lower carrier to interference ratio (C/I=−10) is shown in Figure 1.5 and 1.6 for Δf=0.8 and 1.2 respectively. One could note that the degradation in SNR increases at specific error probability as the carrier to interference ratio decreases.

1.4 Signal to Mean-Square Crosstalk Measure

In this section, we will present a numerical evaluation of the signal to mean-square crosstalk as a performance measure for various modulation schemes and among different MSK-type receiver filters. The derivation of the mean-square crosstalk has been based on the following assumptions:

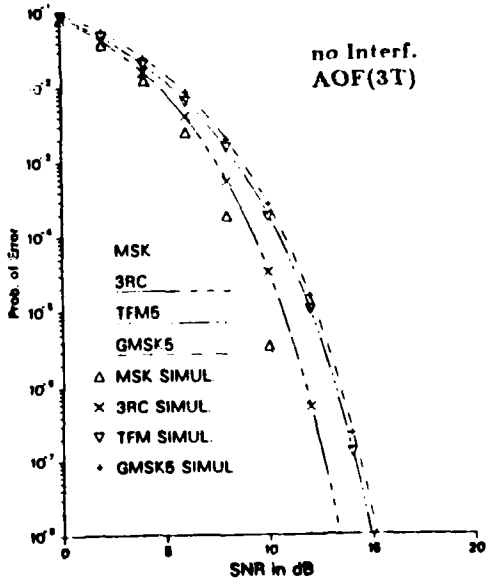

Figure 1.1 The theoretical error probability for various CPM schemes

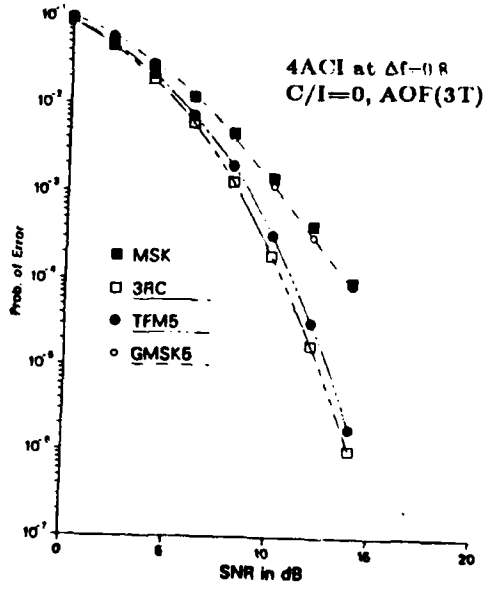

Figure 1.2 Error probability in the presence of ACI, (k=4), at Δf=0.8, for the AOF(3T) receiver.

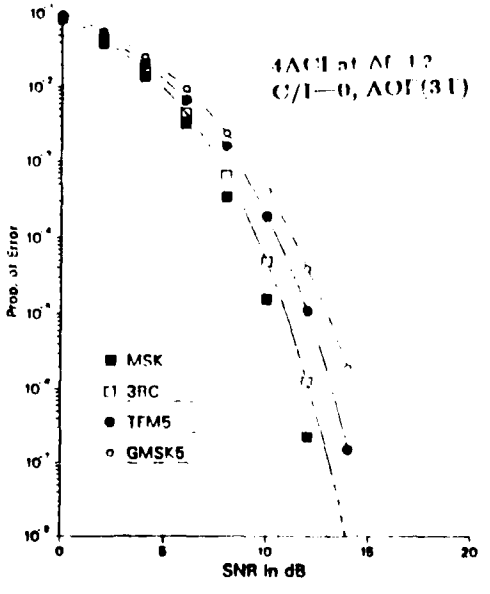

Figure 1.3 Error probability in the presence of ACI, (k=4), at Δf=1.2, for the AOF(3T) receiver.

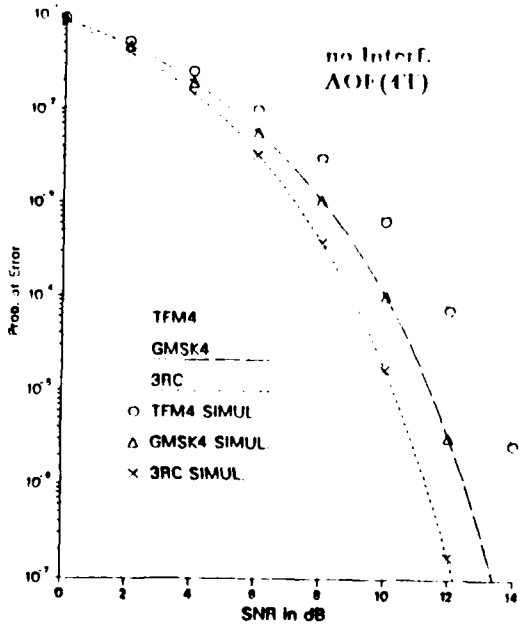

Figure 1.4 The theoretical error probability for various CPM schemes at a larger receiver observation length.

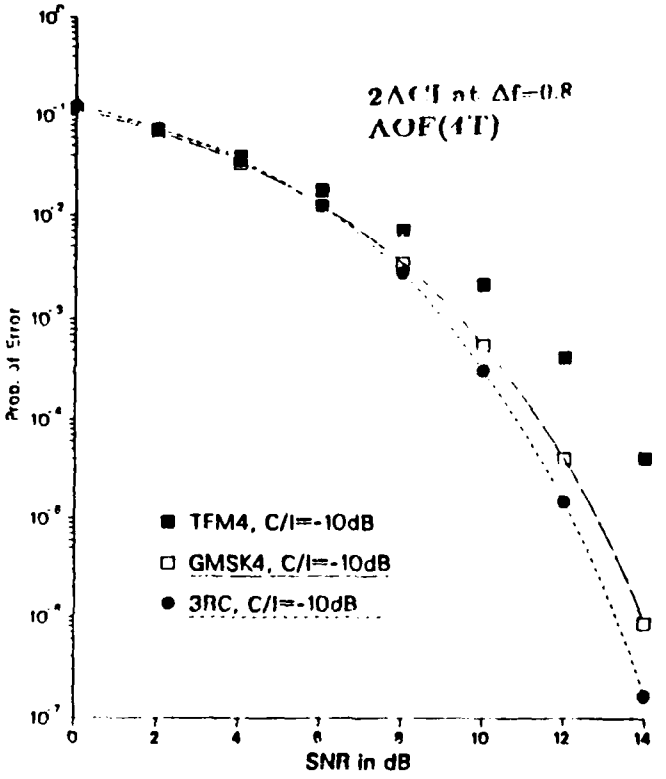

Figure 1.5 Error probability for various CPM schemes in the presence of ACI. (k=2), at lower values of C/I, Δf=0.8.

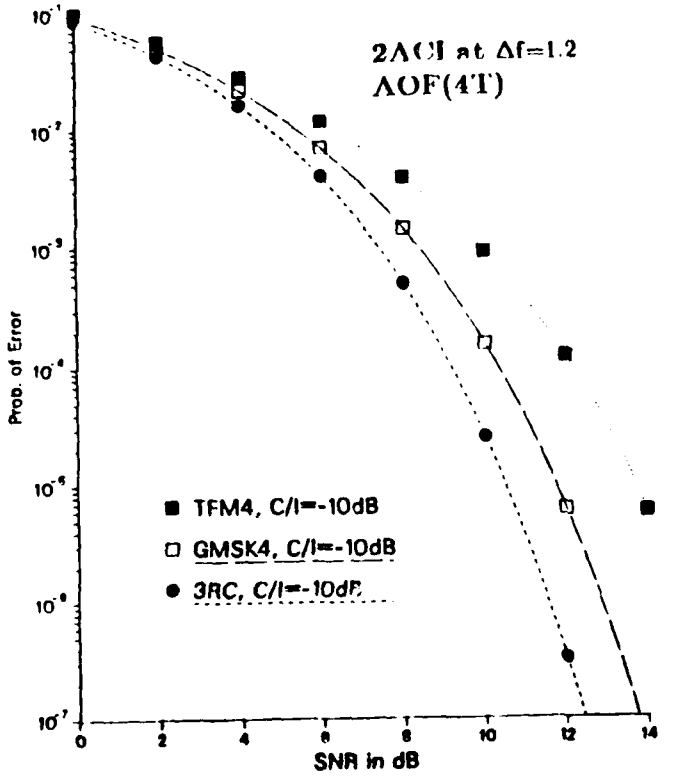

Figure 1.6 Error probability for various CPM schemes in the presence of ACI, (k=2), at lower values of C/I, Δf=1.2.

1. The carrier to interference ratio is unity.
2. No intersymbol interference other than the one caused by the modulation scheme.
3. The interfering signal is stationary.
4. No special processing, such as filtering or data windowing, is applied.

The mean-square crosstalk [8] is defined as

$$\chi = E_{\tau,\beta,\varsigma}\left[x^2_I(\tau, \beta, \varsigma)\right] \tag{1.10}$$

Where E is the expected value. The signal to mean-square crosstalk can be evaluated numerically by

$$SC_TR = \frac{x^2_i/(d_i^2/2)}{\chi} = \frac{E}{\chi} \tag{1.11}$$

where

$$\chi = \frac{\nu^2 E}{T^2} E_\beta \int_0^T \left[\int_{-kT}^{kT} \cos\left(B(t)\right) a(t+\tau)\, dt \right]^2 + \left[\int_{-kT}^{kT} \sin\left(B(t)\right) a(t+\tau)\, dt \right]^2 d\tau \tag{1.12}$$

and

$$B(t) = \left(\Delta\omega t + \psi(t, \beta)\right) \tag{1.13}$$

By using (1.11), we were able to compute the signal to mean-square crosstalk ratio numerically as a function of channel spacing. The numerical results among a selected set of receiver filters for 3RC, TFM(5T), and GMSK(5T) schemes [11] are illustrated in tables 1.1 through 1.3 respectively.

Table 1.1. Signal to mean-square crosstalk ratio in a CPM system employing a 3RC scheme.

Filter Kind	Filter Length	Channel Spacing				
		0.4	0.8	1.2	1.6	2.0
MSK		4.76	18.10	28.90	35.72	39.27
AOF	5T	5.21	21.81	35.81	43.10	46.50
MSEOF	5T	5.24	22.90	40.45	55.45	62.91
AMF	4T	5.31	24.09	45.82	66.91	76.27

Table 1.2. Signal to mean-square crosstalk ratio in a CPM system employing a TFM5 scheme.

Filter Kind	Filter Length	Channel Spacing				
		0.4	0.8	1.2	1.6	2.0
AOF	4T	5.26	22.37	29.95	32.56	34.55
MSEOF	4T	5.34	24.63	35.49	47.21	53.86
AMF	4T	5.43	25.92	41.08	58.37	67.13

Table 1.3. Signal to mean-square crosstalk ratio in a CPM system employing a GMSK4 scheme.

Filter Kind	Filter Length	Channel Spacing				
		0.4	0.8	1.2	1.6	2.0
AOF	5T	5.30	24.52	39.02	44.23	47.46
MSEOF	5T	5.42	25.62	42.08	57.67	65.24
AMF	4T	5.76	26.41	47.62	68.27	78.13

The signal to mean-square crosstalk has also been evaluated by computer simulation of Equation 1.10. Both the numerical and the simulated results are well correlated and are shown in Figures 1.7 to 1.9 for 3RC, TFM(5T), and GMSK(4T) schemes respectively.

The three figures show the signal to mean-square crosstalk ratio (SC_TR) against channel spacing among a selected set of MSK-type receiver filters for three partial response CPM schemes. It was found that AMF(4T) and MSEOF(5T) receivers have a substantial improvement in SC_TR with respect to AOF(4T) and MSK receivers at all channel spacings. Figure 1.7 shows that the MSK receiver performs the worst in the SC_TR measure and it was shown in the previous section that the same receiver filter degrades the most in the error

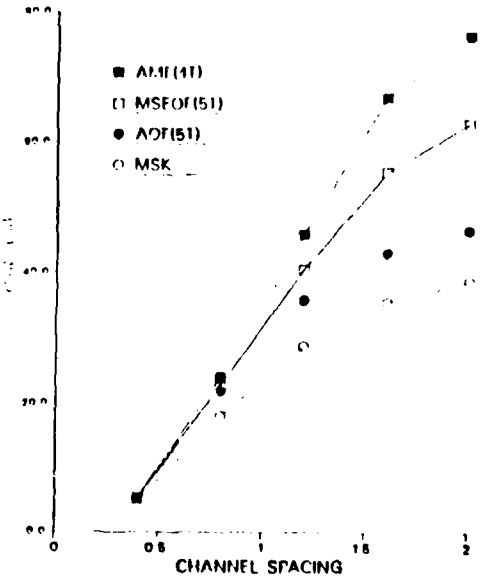

Figure 1.7 ACI rejection of MSK-type receivers for a 3RC scheme.

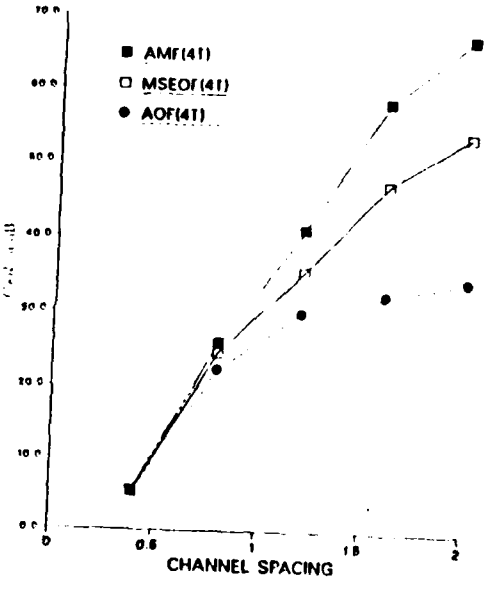

Figure 1.8 ACI rejection of MSK-type receivers for a TFM5 scheme.

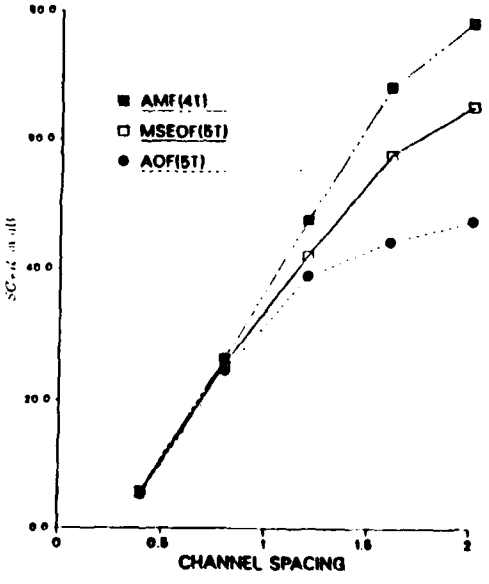

Figure 1.9 ACI rejection of MSK-type receivers for a GMSK4 scheme.

probability measure with interfering signals. While the AOF receiver does not have as good signal to crosstalk performance as the AMF receiver, it has the best error performance among all other receiver filters in the interfering environment. One last observation is that although the MSEOF receiver is inferior in error performance with interfering signals to the AOF receiver, it has a much better rejection of crosstalk than the AOF receiver at all channel spacings. This has been analyzed for three modulation schemes as seen in the last three figures.

1.5 Discussion and Conclusions

In this chapter, the interferences have been modeled as adjacent channel interference and co-channel interference. The first model was considered with the effect of two and four interferers (k=2,4) on the probability of error. It was found that the MSK scheme has optimum performance in the absence of ACI and degrades the most in the presence of ACI. It was also observed that some PRCPM schemes like GMSK5 degrade as badly as MSK at closer channel spacing (Δf=0.8), while 3RC and TFM5 both have a very good rejection of ACI at all channel spacings for AOF(3T). One more important observation; it is not always true that the error performance improves at a larger receiver observation length. This result can be seen in Figures 1.1 and 1.4. So, one may conclude that large improvements can be obtained if the detector filter length is selected appropriately. It was also shown that PRCPM schemes have much lower sidelobes in relation to full response scheme (MSK). These results have made PRCPM schemes popular in bandlimited frequency reuse mobile radio systems, especially when large system capacity is desired.

It was found that the AMF and MSEOF receivers perform substantially better than the AOF and MSK receivers for 3RC and perform better than AOF for TFM5 and GMSK4 schemes. This means that the AMF and MSEOF receivers have a better rejection of ACI at all channel spacings in comparison to the AOF receiver employing PRCPM schemes. One concludes that in order to choose the suitable receiver filter for a specific application, one must compromise between the error performance and the crosstalk performance.

CHAPTER 2

SPACE DIVERSITY OF CPM OVER RAYLEIGH FADING CHANNELS WITH INTERFERING SIGNALS

2.1 Introduction

In a mobile radio environment, the signal transmitted between a fixed base station and a moving radio unit signal suffers from fading and interference. Fading is caused due to multipath transmission. There are also two sources of interferences in this environment. The first source of interference is the ACI and the second source of interference is the CCI. These interferences and fading represent a major source of degradation. Diversity combining is one of the techniques that can be applied successfully to combat fading and reduce interference.

In the next section, we will consider how different envelopes of fading signals can describe the transmitted channel.

2.2 CPM over Rayleigh Fading Channel

In this section an independent slow Rayleigh fading channel is assumed. The error probability for large signal-to-noise ratios is derived for CPM over Gaussian and Rayleigh fading channels. Also, the error probability is shown for Rayleigh fading channels with interfering signals.

2.2.1 Error Probability on Rayleigh Fading Channels

The fading signal s(t) is assumed to follow the Rayleigh density function [2] given by

$$f(s) = \frac{2}{\Omega} s\, e^{-s^2/\Omega} \tag{2.1}$$

where Ω is the instantaneous signal and is given by

$$\Omega = \langle s^2 \rangle . \tag{2.2}$$

The instantaneous SNR can be written as

$$\nu = \frac{s^2}{N_o} \tag{2.3}$$

where N_o is the spectral height of the one-sided Gaussian noise. By substituting (2.3) and (2.2) into (2.1), one can get the pdf of ν as

$$f(\nu) = \frac{1}{\Gamma} e^{-\nu/\Gamma} \quad , \quad \nu \geq 0 \tag{2.4}$$

where Γ is the average SNR and is defined by

$$\Gamma = \frac{\Omega}{N_o} = \left\langle \frac{s^2}{N_o} \right\rangle . \tag{2.5}$$

The average error probability of the modulation scheme with coherent detection can be written as:

$$P(\nu) = \sum_{i=1}^{m} c_i Q\left(\sqrt{d_i^2 \nu}\right) \tag{2.6}$$

where $Q(\cdot)$ is the error function associated with the normal distribution d_i^2 is the squared Euclidean distance associated with a signal corresponding to data sequence number i received in the fixed filter, and c_i is the probability of that specific signal. m is the total number of sequences. Assuming independent data symbols with equal probability, then

$$c_i = \frac{1}{m} . \tag{2.7}$$

The average bit-error probability in the fading case is

$$P = \int_0^{\infty} P(\nu) f(\nu) \, d\nu \tag{2.8}$$

where $P(\nu)$ and $f(\nu)$ are given by (2.6) and (2.4) respectively. Using (2.6) and (2.4) in (2.7) one can obtain

$$P = \frac{1}{2m} \sum_{j=1}^{m} \left[1 - \sqrt{\frac{d_j^2 \Gamma/2}{1 + d_j^2 \Gamma/2}} \right] . \tag{2.9}$$

From (2.9) one can evaluate the bit-error probability over a Rayleigh fading channel for CPM schemes. Figure 2.1 shows the error probability for 3RC, TFM4, and GMSK4 schemes employing an AOF(4T)

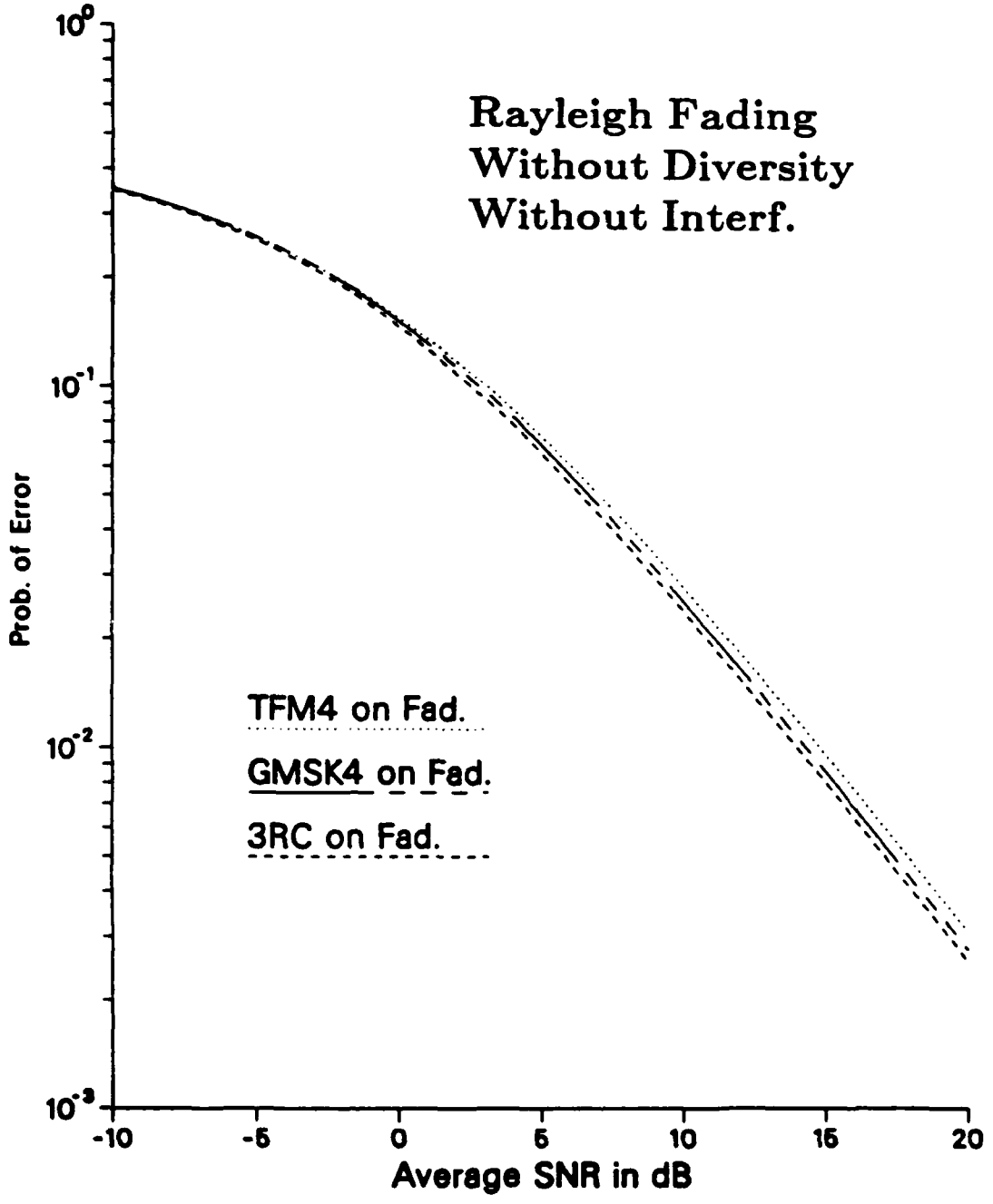

Figure 2.1 Error probability P vs. average SNR Γ for various selected binary CPM schemes, h=1/2, employing an AOF(4T) receiver.

receiver on Gaussian and Rayleigh fading channels.

2.2.2 An Easy Way to Evaluate the Error Performance With Interfering Signals

In this section, we develop an easy method to evaluate the error probability in the interfering environment. This method might not be as accurate as the simulation technique used previously but it is much faster from the computational point of view. The analysis here is based on stationary white Gaussian noise with power spectral density N_o.

The algorithm is mainly an evaluation of the normalized squared Euclidean distance of the desired and interfering signals. For the desired signal, the normalized squared Euclidean distance is calculated from:

$$d_j^2 = \frac{\frac{2}{T}\left[\int_I a(-t)\,\tilde{s}(t,\alpha_j)\,dt\right]^2}{\int_I a^2(t)\,dt}. \tag{2.10}$$

For the interfering case, the normalized squared Euclidean distance is computed numerically. It is also computed by computer simulation of the filter output due to each interfering channel. The filter output due to the jth interfering channel is

$$x_{I_j}(\tau_j,\beta_j,\varsigma_j) = \sqrt{\frac{2E}{T}}\,\nu_j\left[a(t) * \cos\left(\omega_j(t-\tau_j) + \psi(t-\tau_j,\beta_j) + \varsigma_j\right)\right] \tag{2.11}$$

The normalized squared Euclidean distance of the jth interferer is defined as $(d_{I_j}^2)$ and is given by

$$d_{I_j}^2 = \frac{\frac{2}{T}\left[x_{I_j}(\tau_j,\beta_j,\varsigma_j)\right]^2}{\int_I a^2(t)\,dt}. \tag{2.12}$$

The overall normalized squared Euclidean distance for the jth sequence is $(d_{j_{ov}}^2)$ and is given by

$$d_{j_{ov}}^2 = d_j^2 - \sum_{i=1}^{k} d_{I_i}^2 \tag{2.13}$$

where $\sum_{i=1}^{k} d_{I_j}^2$ represents the normalized squared Euclidean distance due to k interferers. The error probability for the interfering case is

$$P(\nu) = \frac{1}{m} \sum_{j=1}^{m} Q\left[\sqrt{d_{jov}^2 \nu}\right] \tag{2.14}$$

where Q is the Gaussian error function and m is the total number of sequences.

It was found that the resulting error probability using this algorithm is the same as the one obtained by the simulation technique used previously with an error rate of less than 5%. This is seen in Figure 2.2 and 2.3 respectively. One could notice in both figures that at lower C/I, i.e., when the desired signal power is weak compared to the interfering signal power, the performance degradation is the highest. Figure 2.4 shows the error performance of a 3RC scheme employing an AOF(4T) receiver with one and multiple CCI at various C/I. It is recognized that the difference in performance degradation due to the interferers is the most at low C/I and it reduces at higher values of C/I. One last observation is that the effect of one CCI and two CCI is almost the same at higher values of C/I, i.e., when the signal power is strong enough the number of co-channel interfering signals will not have much effect on the system performance.

2.2.3 Error Performance over Fading Channels with Interfering Signals

In this section, we will evaluate the error probability when the signal is combined with fading and interference. It is assumed that fading due to the interfering channels is negligible compared to fading due only to the desired channel. The average bit error probability in this case is obtained by substituting (2.4) and (2.12) in (2.8). The result is

$$P = \frac{1}{2m} \sum_{j=1}^{m} \left[1 - \sqrt{\frac{d_{jov}^2 \Gamma/2}{1 + d_{jov}^2 \Gamma/2}}\right]. \tag{2.15}$$

Figure 2.5 shows the error probability for the 3RC scheme on fading and both ACI and CCI with various C/I. One may notice, that the signal affected by CCI and fading has larger C/I than that affected by ACI and fading even at closer channel spacings. This is predictable because CCI has more influence on performance degradation than ACI due to it is existence within the same signal bandwidth. Figure 2.6 illustrates the same result for various CPM schemes under the

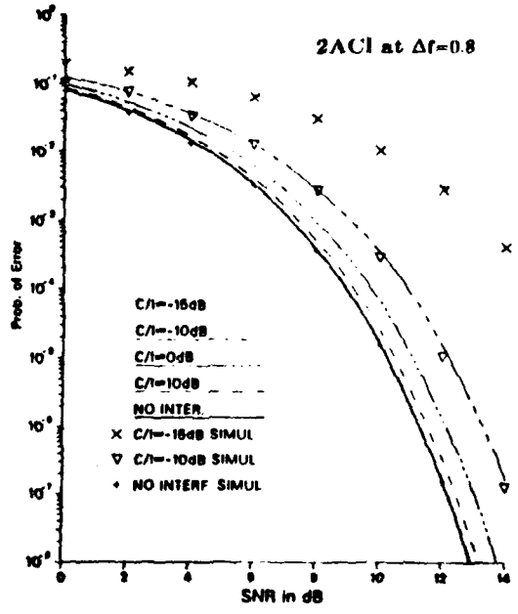

Figure 2.2 Effect of carrier to interference ratios C/I's on error probability for a 3RC scheme employing an AOF(4T) receiver.

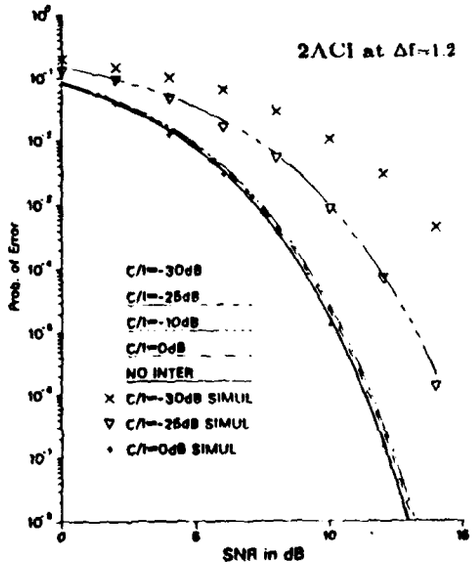

Figure 2.3 Effect of carrier to interference ratios C/I's on error probability for a 3RC scheme employing an AOF(4T) receiver.

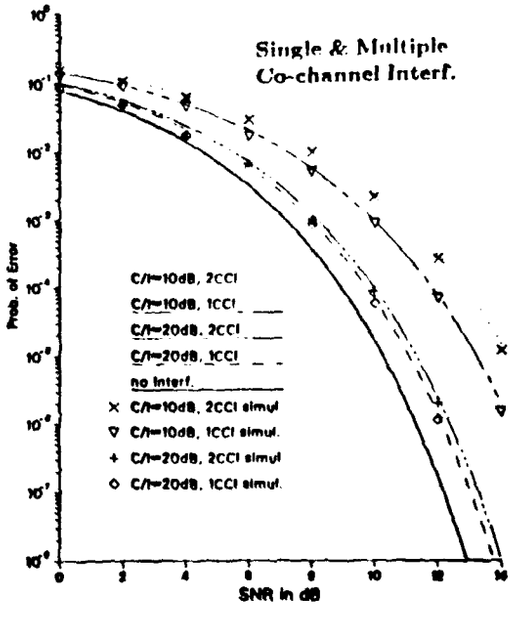

Figure 2.4 Effect of single and multiple co-channel interference CCI, with various C/I's, on error probability for a 3RC scheme using an AOF(4T).

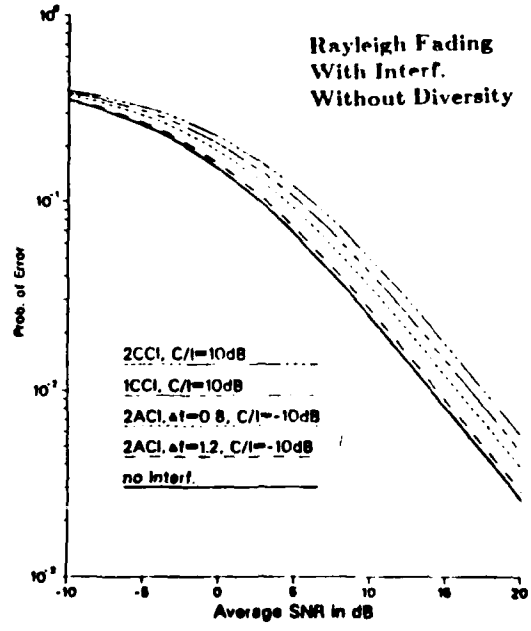

Figure 2.5 Error probability P vs. average SNR Γ for a 3RC scheme and various kinds of interfering signals, employing an AOF(4T) receiver.

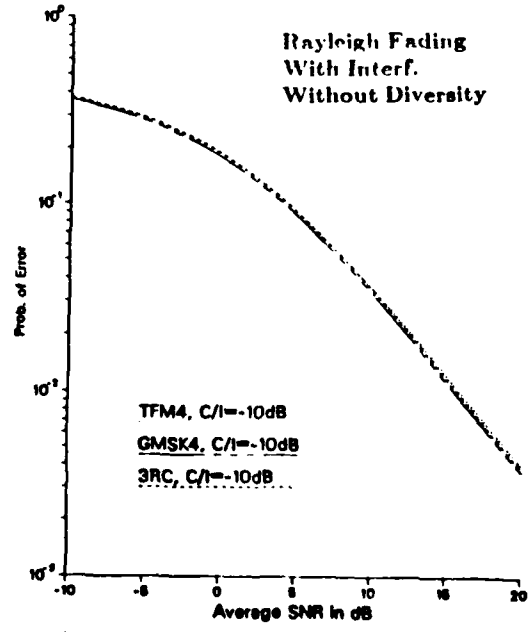

Figure 2.6 Error probability P vs. average SNR Γ for various selected h=1/2, binary CPM schemes with an AOF(4T) receiver.

influence of ACI and channel spacing of 0.8 the bit rate.

2.3 Diversity Approach for CPM with Interfering Signals

Space diversity is an effective weapon against the cochannel interference encountered in cellular mobile radio systems. High order diversity and strong interference suppression can be achieved with modest hardware complexity by using diversity combining techniques.

In the next section, we will consider ideal maximal ratio combining as an alternative technique to combat fading and reduce interference.

2.3.1 Error Performance of CPM for Ideal MRC With Independent Diversity Branches

For independent diversity branches, there is an independent Rayleigh fading in each branch, while for ideal maximal ratio combining the receiver must know each path magnitude and phase to perform perfect combining. It must also have the property that the output SNR is the sum of the instantaneous branch SNRs, i.e.,

$$\nu = \sum_{k=1}^{M} \nu_k \tag{2.16}$$

where M is the number of diversity branches, ν_k is the instantaneous SNR at the kth branch. The fading signal s(t) at the kth branch is assumed to follow the Rayleigh density function, i.e.,

$$f(s) = \frac{2}{\Omega_k} s\, e^{-s^2/\Omega_k} \tag{2.17}$$

where

$$\Omega_k = \left\langle s_k^2 \right\rangle . \tag{2.18}$$

The instantaneous SNR at the kth branch is given by

$$\nu_k = \frac{s_k^2}{N_o} . \tag{2.19}$$

Hence, the p. d. f. of ν_k is

$$f(\nu_k) = \frac{1}{\Gamma_k} e^{-\nu_k/\Gamma_k} \tag{2.20}$$

where Γ_k is the average SNR per the kth branch and is considered equally among all branches. i.e.,

$$\Gamma_k = \Gamma. \tag{2.21}$$

In this case, the p.d.f. of ν is obtained by substituting (2.21) and (2.16) into 5.16, hence

$$f(\nu) = \frac{M}{\Gamma} \left(\frac{\nu}{\Gamma}\right)^{M-1} \frac{1}{(M-1)!} e^{-\nu/\Gamma} \tag{2.22}$$

for M-branch MRC, assuming independent Rayleigh fading in each branch. The average receiver output SNR is

$$E(\nu) = M\,\Gamma. \tag{2.23}$$

The bit error probability for the MRC diversity case, for PRCPM with coherent MSK-type reception [3], is obtained by substituting (2.22) and (2.7) in (2.8) and is given by

$$P = \frac{1}{2m} \sum_{i=1}^{m} \left[1 + \sqrt{\frac{d_i^2\Gamma/2}{1+d_i^2\Gamma/2}} \left\{1 + \frac{1}{1!2}(1+\frac{d_i^2\Gamma}{2})^{-1}\right\}\right]$$
$$+ \frac{1.3}{2!2^2}(1+\frac{d_i^2\Gamma}{2})^{-2} + \ldots\ldots +$$
$$\left[\int_0^0 \left\{\frac{1.3.5\ldots\ldots(2M-3)}{(M-1)!\,2^{(M-1)}}(1+\frac{d_i^2\Gamma}{2})^{-(M-1)}\right\}\right]. \tag{2.24}$$

Numerical calculations of (2.24) for various modulation schemes over an AOF(4T) receiver are shown for 2 and 4 branches in Figure 2.7. One may notice the improvement in error probability versus the average per branch signal-to-noise ratio (Γ) for various modulation schemes by using more diversity branches.

The case of diversity against both fading and interference can be evaluated numerically by replacing the normalized squared Euclidean

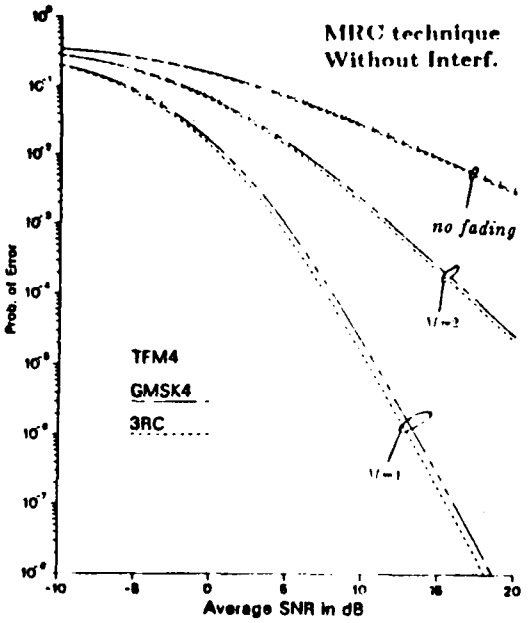

Figure 2.7 Error probability P vs. average-per-branch SNR Γ for various h=1/2, binary CPM schemes with an AOF(4T) receiver and M-branch diversity with maximal-ratio combining.

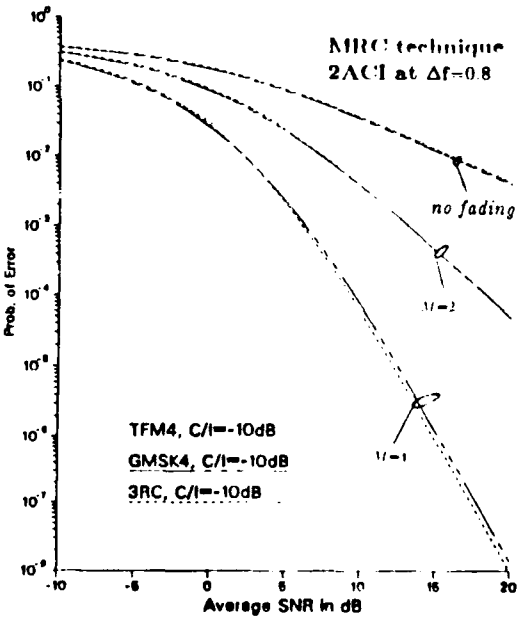

Figure 2.8 Error probability P vs. average-per-branch SNR Γ for various h=1/2, binary CPM schemes with an AOF(4T) receiver and M-branch diversity with maximal-ratio combining.

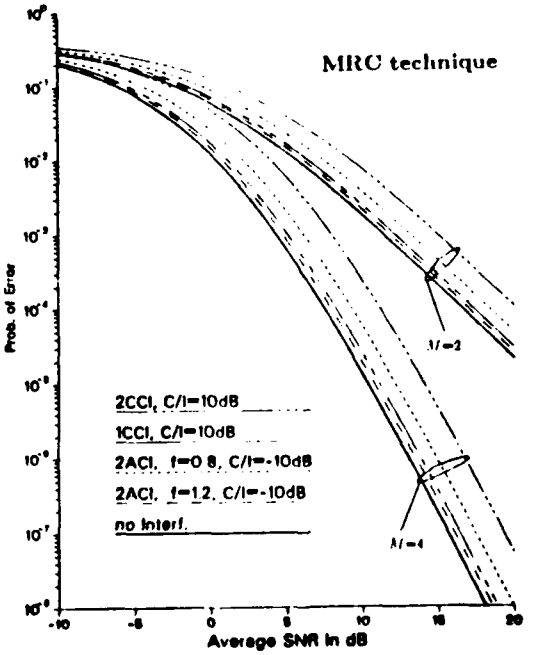

Figure 2.9 Error probability P vs. average-per-branch SNR Γ for a 3RC with various kinds of interfering signals, M-branch diversity with maximal-ratio combining, employing an AOF(4T) receiver.

distance (d_j^2) in (2.24) by the overall normalized squared Euclidean distance (d_{jov}^2) in (2.13). Figure 2.8 shows the numerical evaluation of space diversity with maximal ratio combining (MRC) technique for the same class of modulation schemes under both fading and interference for 2 and 4 diversity branches. A little performance degradation can be seen compared to Figure 2.7 due to the consideration of the interference. Figure 2.9 illustrates the performance improvement by using the MRC technique with 2 and 4 diversity branches, over that of Figure 2.5.

2.3.2 Error Performance of CPM for Ideal SRC with Independent Diversity Branches

For the ideal selection ratio combining technique the combiner selects the diversity branch which has the largest SNR for bit decisions. The same branch is used for all symbols over one time interval for the receiver filter under the assumption of slow fading. For Rayleigh fading, the instantaneous SNR in the kth branch (ν_k) has the p. d. f. shown in (2.20). The output SNR (ν) is equal to

$$\nu = \text{max. } (\nu_1, \nu_2, \ldots, \nu_k, \ldots, \nu_M) \tag{2.25}$$

where M is the total number of branches. The probability density function for ν [2] is

$$f(\nu) = \frac{M}{\Gamma} e^{-\nu/\Gamma} (1 - e^{-\nu/\Gamma})^{M-1} \tag{2.26}$$

where Γ is the average SNR per branch. The average receiver output SNR in this case is

$$E(\nu) = \Gamma \sum_{k=1}^{M} \frac{1}{k} \tag{2.27}$$

which of course increases more slowly with increasing M than the corresponding average for MRC (2.23). Sundberg [2] derived the average bit error probability for BPSK, M branch diversity with selection combining. For CPM the derivation is similar. The derivation is considered under the assumption of coherent detection of MSK-type receivers. The average bit error probability in this case is given by

$$P = \frac{1}{2m} \sum_{i=1}^{m} \sum_{j=0}^{M} \frac{(-1)^j \binom{M}{j}}{\sqrt{1 + 2 \frac{j}{d_i^2} \Gamma}} \tag{2.28}$$

where d_i^2, i=1, ..., m is defined by the modulation scheme and by the receiver filter. Numerical evaluation of (2.28) for the same set of modulation schemes over an AOF(4T) receiver is illustrated for 2 and 4 diversity branches in Figure 2.10. The case of the SRC diversity technique against both fading and interference is evaluated numerically by replacing the normalized squared Euclidean distance (d_j^2) in (2.28) by (d_{jov}^2) in Equation 2.13. Figure 2.11 shows the error probability in the interfering environment using different diversity branches with the selection ratio combining technique.

In the preceding section the analysis has been based on the assumption that the fading signals in the various branches are uncorrelated. It is important to examine the possible deterioration of performance of a diversity system when the branch signals are correlated.

2.3.3 Error Performance of CPM Using MRC with Correlated Branches (M=2)

In the derivation of this part, the average SNR's are assumed the same in both branches. Accordingly, the fading envelope will take the form [52];

$$f(s) = \frac{2\sqrt{\pi}}{(1-\rho)}\left(\frac{1}{\Omega}\right)^2 s \exp -\left\{\frac{s^2}{\Omega(1-\rho)}\right\} \cdot \left\{\frac{\Omega(1-\rho)s^2}{2\sqrt{\rho}}\right\}^{1/2} I_{1/2}\left\{\frac{\sqrt{\rho}s^2}{\Omega(1-\rho)}\right\} \qquad (2.29)$$

where ρ is the power correlation coefficient between branches such that $0 \leq \rho \leq 1$. $I_{1/2}(.)$ is the 1/2 order modified Bessel function of the first kind.

By making the substitution of $\nu = s^2/N_o$ in (2.29), one gets

$$f(\nu) = \frac{\sqrt{\pi}}{\Gamma} e^{-\frac{\nu}{\Gamma(1-\rho)}} \left\{\frac{\nu}{2(1-\rho)\sqrt{\rho}\Gamma}\right\}^{1/2} I_{1/2}\left\{\frac{\sqrt{\rho}}{\Gamma(1-\rho)}\nu\right\}. \qquad (2.30)$$

The bit error probability is given by;

$$P = \frac{1}{2m}\sum_{i=1}^{m}\left\{1 - \frac{1}{2\sqrt{\rho}}\left[\sqrt{\frac{(1+\sqrt{\rho})}{1+\frac{2}{d_i^2\Gamma(1+\sqrt{\rho})}}}\right]\right\}$$

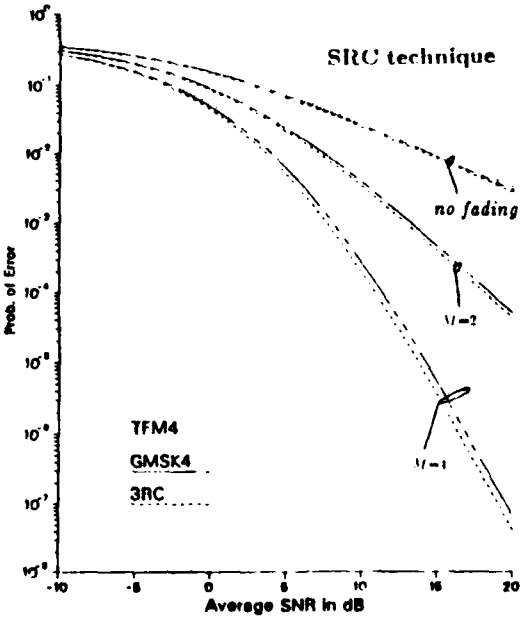

Figure 2.10 Error probability P vs. average-per-branch SNR Γ for a 3RC with an AOF(4T) receiver and M-branch diversity with selection combining.

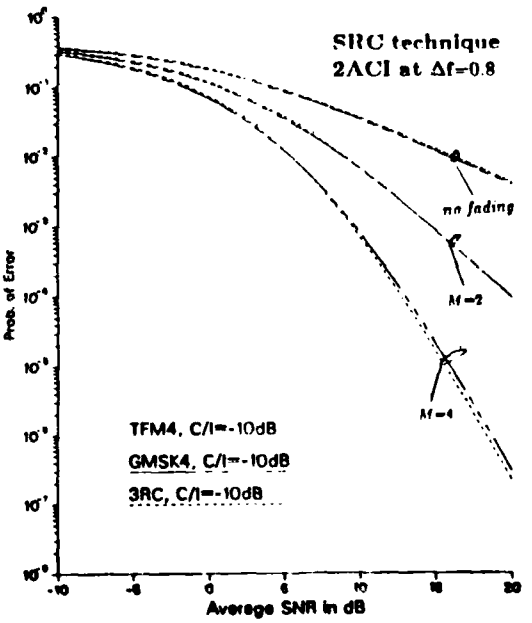

Figure 2.11 Error probability P vs. average-per-branch SNR Γ for a 3RC scheme with an AOF(4T) receiver and M-branch diversity with selection combining.

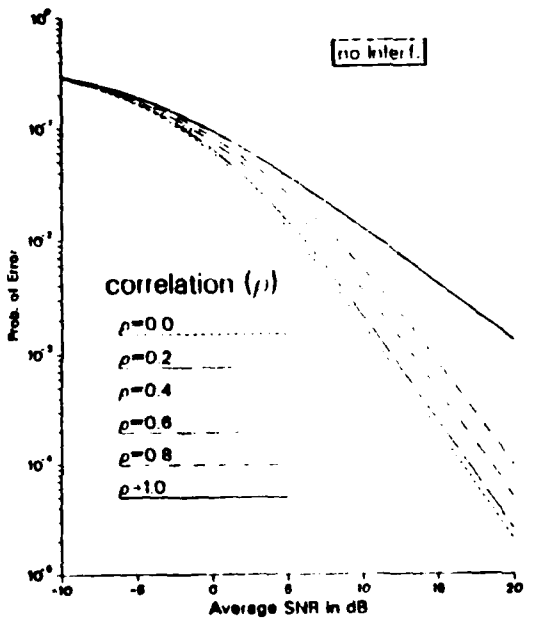

Figure 2.12 Effect of correlation among diversity branches (M=2) with the MRC technique on the error probability, 3RC scheme employing an AOF(4T) receiver.

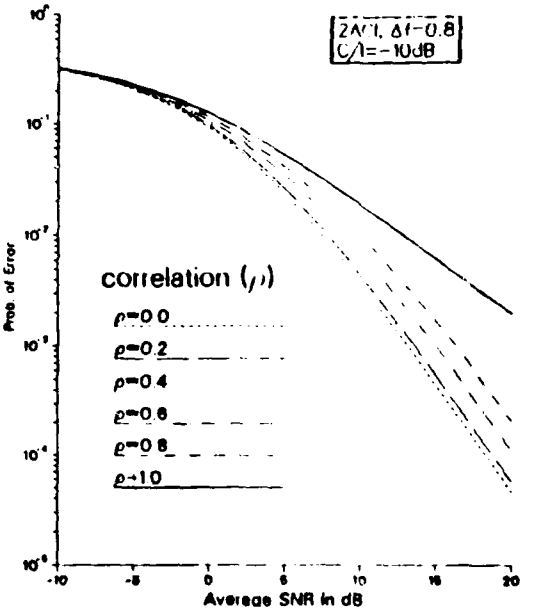

Figure 2.13 Effect of correlation among diversity branches (M=2) with the MRC technique on the error probability, 3RC scheme with adjacent channel interference, employing an AOF(4T) receiver.

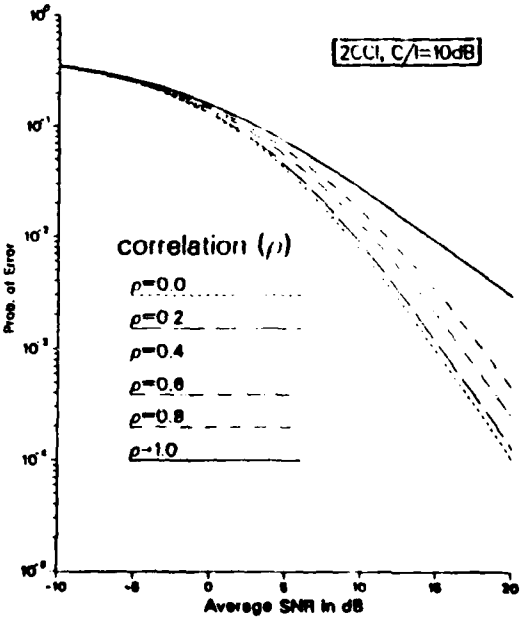

Figure 2.14 Effect of correlation among diversity branches with the MRC technique on the error probability, 3RC scheme with co-channel interfering, employing an AOF(4T) receiver.

$$- \left\{ \left[\sqrt{\frac{(1-\sqrt{\rho})}{1+\frac{2}{d_i^2\Gamma(1-\sqrt{\rho})}}} \right] \right\}. \tag{2.31}$$

It is obvious that the last expression is valid for all permissible values of ρ except at $\rho=0$.

Limiting Case ($\rho=0$)

By using the ascending series of the modified spherical Bessel function [14] for small argument in the form

$$\sqrt{\frac{1}{2}\pi/z}\, I_{n+1/2}(z) = \frac{z^n}{1.3.5....(2n+1)} \cdot \left\{ 1 + \frac{z^2/2}{1!(2n+3)} + \frac{(z^2/2)^2}{2!(2n+3)(2n+5)} + ... \right\} \tag{2.32}$$

the bit error probability can be developed. One may notice that the argument of I(.) is zero in our case, so the above expression suits our situation perfectly. The average bit error probability in this case is given by

$$P = \frac{(1-\rho)}{2m} \sum_{i=1}^{m} \left[1 - \frac{2+3/\gamma_i}{2(1+1/\gamma_i)^{3/2}} \right] \tag{2.33}$$

where

$$\gamma_i = \frac{d_i^2\Gamma(1-\rho)}{2}. \tag{2.34}$$

Figure 2.12 shows the effect of correlation, among diversity branches with maximal ratio combining technique, on the error probability for the 3RC scheme. Figures 2.13 and 2.14 illustrate the same effect of the correlation while taking into consideration the influence of the adjacent channel interference and co-channel interference on the error performance respectively.

2.4 Conclusions

In this chapter, the problem of the interfering channels in Rayleigh fading environment with diversity reception for partial response continuous phase modulation (PRCPM) schemes was addressed.

PRCPM schemes with various kinds of interfering signals on Rayleigh fading channels perform very poorly and a bit error probability of 10^{-3} was unattainable at SNR of 20 dB. By introducing the diversity combining approach with the maximal ratio combining technique, even with only two diversity branches, the error performance tremendously improved. By using diversity with the selection combining technique the error probability could be improved in the same manner but with less improvement than the one accomplished by using the maximal ratio combining technique. This means that the results obtained from this chapter reduce to the classical results for the case of no interference.

REFERENCES

[1] I. Kalet, "A Look at Crosstalk in Quadrature-Carrier Modulation Systems," *IEEE Trans. on Commun.*, Vol. COM-25, No. 9, pp. 884-892, September 1977.

[2] M. Schwartz, W. Bennett and S. Stein, *Communication Systems and Techniques*, N. Y.: McGraw - Hill Book Co., 1966.

[3] C. E. Sundberg, "Error Probability of Partial Response Continuous Phase Modulation with Coherent MSK-Type Receiver, Diversity and Slow Rayleigh Fading in Gaussian Noise," *Bell Syst. Tech. J.*, Vol. 61, pp. 1933-1963, October 1982.

[4] F. De jager and C. B. Dekker, "Tamed Frequency Modulation, A Novel Method to Achieve Spectrum Economy in Digital Transmission," *IEEE Trans. Commun.*, Vol. COM-26, pp. 534-542, May 1978.

[5] K. Murota and K. Hirade, "GMSK Modulation for Digital Mobile Radio Telephony," *IEEE Trans. Commun.*, Vol. COM-29, pp. 1044-1050, July 1981.

[6] T. Aulin, C. E. Sundberg and A. Svensson, "MSK-Type Receivers for Partial Response Continuous Phase Modulation," *Int. Conf. Commun.*, Philadelphia, PA, pp. 6F3.1-6, Jun. 1982.

[7] B. E. White, "A Worst-Case Crosstalk Comparison Among Several Modulation Schemes," *IEEE Trans. Commun.*, Vol. COM-25, No. 9, pp. 1032-1037, Sep 1977.

[8] V. Varma and S. C. Gupta, "Performance of Partial Response CPM in the Presence of Adjacent Channel Interference and Gaussian Noise," *IEEE Trans. on Commun.*, Vol. COM 34, No. 11, Nov. 1986.

[9] W. Refai and S. C. Gupta "Performance Evaluation of Partial Response CPM with Optimum MSK-Type Receivers in the Presence of ACI," *VTC 1987*, June 1-3, Tampa, Florida.

[10] T. Aulin and C. E. Sundberg, "An Easy Way to Calculate Power Spectra for Digital FM," *IEE Proc.*, Vol. 130, part F, No. 6, pp. 519-526, Oct. 1983.

[11] W. Refai and S. C. Gupta "Performance Analysis for CPM with MSE Optimum Detector in a Mobile Gaussian Channel with Interfering Signals," *VTC 1988* June 14-17, Philadelphia, PA.

[12] W. Refai and S. C. Gupta, "Space Diversity of CPM over Fading Channels with Interfering Signals," *Int. Conf. Commun.*, Philadelphia, PA, June 1988.

[13] M. Nakagami, "The m-distribution. A General Formula of Intersity Distribution of Rapid Fading," *Statistical Methods of Radio Wave Propagation*, Pergamon Press, 1960.

[14] M. Abramowitz and I. A. Stegun, "Handbook of Mathematical Functions" *Appl. Math. Series 55*, National Bureau of Standards, 1964.

[15] F. Amoroso, "The Bandwidth of Digital Data Signals," *IEEE Commun. Magazine*, pp. 13-24, Nov. 1980.

CHAPTER 3

ADAPTIVE MULTIPATH DIVERSITY RECEIVERS

3.1 Introduction

The number of terminals for indoor use has grown considerably over the years. An emerging concept is to provide wireless communication between these terminals. Indoor wireless communication is hampered by a severe multipath problem. This multipath propagation manifests as Intersymbol Interference (ISI) and frequency selective fading. For indoor channel applications where the symbol duration is much larger than the multipath spread, frequency selective fading is the major error causing mechanism. Since the errors in symbol detection occurs due to envelope fading diversity can be used to mitigate the effect. By using Direct Sequence Spread Spectrum (DSSS) signaling multipath diversity can be used to combat fading. The DSSS signal resolves the multipath to provide uncorrelated replicas of the transmitted signal at the receiver. The receiver is designed to demodulate each replica independently to attain diversity gain. This chapter is concerned with the formal development of a class of known delay adaptive multipath diversity receivers and the evaluation of their p;erformance. The receiver is *adaptive* in the sense that it periodically measures channel characterizing parameters (path gains and phase shifts) and uses these estimates for signal detection.

The receiver structure is derived as a generalization of [4] and [5] for a frequency selective fading quasi-static channel. This formulation is appropriate only for channels with multipath spread less than the signaling symbol duration, such as an indoor wireless communication link. No restriction is placed on the shape of the multipath delay power profile of the channel. Orthogonal and phase coded signaling are considered. Finally, an attempt is made to obtain closed form expressions for bit error probability.

3.2 Receiver Structure for Binary Orthogonal Signaling

The received signal, in the symbol interval $(L-1)T \leq t \leq LT$, under the two hypotheses $(H_i,\ i = 0, 1)$ can be expressed as in [13]:

$$H(L) = H_i \ : \ r(t) = \sum_{k=1}^{N_c} C_k(L)\, A\, p_i(t_1 - kT_p) + z(t) \qquad (3.1)$$

where $t_1 = t - (L-1)T$. $p_i(t)$ is the DSSS code. A is the signal

amplitude. z(t) is an additive zero mean complex Gaussian noise process with autocorrelation function $\phi_z(t, \tau) = N_o\, \delta(t - \tau)$. The noise is assumed uncorrelated with the message sequence and the C_k' s.

(i) Vector Characterization of Received Signal

The first step in the receiver formulation is to obtain a vector characterization of the received signal over each signaling interval. This is done by defining the following set of orthonormal basis functions:

$$b_k(t) = \begin{cases} \dfrac{1}{\sqrt{E_p}}\, p_1(t - kT_p) & k = 1, 2, \ldots, N_c \\ \dfrac{1}{\sqrt{E_p}}\, p_0(t - \overline{k-N_c}\, T_p) & k = N_c+1, \ldots, 2N_c \\ b_k'(t) & k > 2N_c \end{cases} \tag{3.2}$$

where $\{b_k'(t),\ k > 2N_c\}$ is an arbitrary orthonormal set of basis functions that are chosen to make the orthonormal set $\{b_k(t),\ k = 1, 2, \cdots\}$ complete. The notation $\overline{k-N_c}$ implies $(k-N_c)$.

The definition of the basis function is based on the ideal assumption that:

$$\int_0^T p_i(t - kT_p)\, p_j(t - mT_p)\, dt = \begin{cases} E_p\, \delta(k-m) & i=j \\ 0 & i \neq j \end{cases} \tag{3.3}$$

Define

$$r_k(L) = \int_{(L-1)T}^{LT} r(t)\, b_k^*(t_1)\, dt \tag{3.4}$$

where $r_k(L)$ is a projection of $r(t)$ along $b_k(t)$ in the time interval $(L-1)T \leq t \leq LT$. $r_k(L)$ is a linear functional of the received signal $r(t)$.

Assuming $T_m \ll T$, ISI can be neglected. Substituting (3.1) and (3.2) in (3.4) and using (3.3), it can be readily shown that under each hypothesis, $(H_i,\ i = 0,1)$, $r_k(L)$ is given by:

$H(L) = H_i$:

$$r_k(L) = \begin{cases} i\, A\sqrt{E_p}\, C_k(L) + z_{kL}^1 & k = 1, 2, \ldots, N_c \\ (i-1)\, A\sqrt{E_p}\, C_{\overline{k-N_c}}(L) + z_{kL}^\circ & k = N_c + 1, \cdots, 2N_c \\ z'_{kL} & k > 2N_c \end{cases} \tag{3.5}$$

where

$$z_{kL}^1 = \int_{(L-1)T}^{LT} z(t)\, \frac{1}{\sqrt{E_p}}\, p_1(t_1 - kT_p)\, dt$$

$$z_{kL}^\circ = \int_{(L-1)T}^{LT} z(t) \frac{1}{\sqrt{E_p}}\, p_o(t_1 - \overline{k-N_c}\, T_p)\, dt$$

$$z'_{kL} = \int_{(L-1)T}^{LT} z(t)\, b'_k(t)\, dt$$

Now, $\{z_{kL}^1, k = 1, 2, \ldots, N_c\}$, $\{z_{kL}^\circ, k = N_c + 1, \ldots, 2N_c\}$ and $\{z'_{kL}, k > 2N_c\}$ are noise terms, which are uncorrelated for all k, L and are identically distributed zero mean complex Gaussian random variables with variance N_o.

Due to the independence of noise terms, z_{kL}^1, z_{kL}° and z'_{kL}, and since the noise terms are uncorrelated with the C_k, it is seen from (3.5) that $\{r_k(L), \quad k = 1, 2, \ldots, 2N_c\}$ form a set of sufficient statistics. This set of sufficient statistics is defined vectorially as $\mathbf{R}(L) = [r_1(L)\ r_2(L) \cdots r_{2N_c}(L)]^T$.

(ii) Definition of Memory Information

It is proposed to use a memory to store the received signal over M_b past symbol durations. This means that at time $t = LT$ all the information available to the receiver, on the complex path gains C_k, is contained in r(t) received over $(L - M_b)T \leq t \leq (L-1)T$. As an alternative, it is possible to store a linear functional of r(t) such as $r_k(L)$. $r_k(L)$ preserves the Gaussian nature of the memory information and all the information on C_k. From (3.5) it is clear that one needs to store only the set of sufficient statistics $\{r_k(j), k = 1, 2, \ldots, 2N_c\}$ over

$(L - M_b) \leq j \leq (L-1)$. It is further observed that each $r_k(j)$ contains an unknown modulation component, viz., which hypothesis H_1 or H_o is true. This unknown component is removed from the memory information, by redefining the basic memory variable as:

$$\text{(i)} \qquad V_k(j) \triangleq \frac{r_k(j) + r_{\overline{k+N_c}}(j)}{2} \tag{3.6}$$

$$\text{(ii)} \qquad V_k(j) \triangleq d_j\, r_k(j) + (1 - d_j)\, r_{\overline{k+N_c}}(j) \tag{3.7}$$

where $d_j = i$ when hypothesis H_i $i = 0,1$, is true in the j^{th} signaling interval. This is a decision feedback scheme, where d_j corresponds to past bit decisions. In (4.5) the division by 2 is done so that the $V_k(j)$ under both schemes has the same noise variance of N_o.

Now, the set of variables $\{V_k(j), k = 1, 2, ..., N_c\}$ collected over the interval $(L - M_b) \leq j \leq (L-1)$ constitutes the memory information that will be stored. $V_k(j)$ are complex Gaussian random variables.

Since the $r_k(j)$ are uncorrelated, the corresponding $V_k(j)$ are also uncorrelated. Hence, the memory information can be partitioned into N_c independent blocks, each of length M_b. The k^{th} block of memory information is designated vectorially as:

$$\mathbf{m}_{kL} = [V_k(L - M_b + 1) \cdots V_k(L-1)]^T \tag{3.8}$$

The total memory information is designated as $\mathbf{I}_L^m$ where $\mathbf{I}_L^m = [\mathbf{m}_{1L}\ \mathbf{m}_{2L} \cdots \mathbf{m}_{N_cL}]$.

Now all the information on the complex channel coefficients, represented vectorially as $\mathbf{C}(L) = [C_1(L)\ C_2(L) \cdots C_{N_c}(L)]^T$, is contained in $\mathbf{I}_L^m$. Thus, the information $\mathbf{C}(L)$ given $\mathbf{I}_L^m$ can be expressed by the conditional density:

$$P(\mathbf{C}(L) \,|\mathbf{I}_L^m) = \prod_{k=1}^{N_c} P(C_k(L) \,|\mathbf{m}_{kL}) \tag{3.9}$$

This expression follows from the uncorrelated scattering assumption for the C_k and the independence of memory blocks. Since, $\mathbf{m}_{kL}$ is a complex Gaussian random vector and it can be shown, [1], [24], that:

$$P(C_k(L) \,|\mathbf{m}_{kL}) = \frac{1}{2\pi\sigma_L^2} \exp(-\frac{|C_k(L) - \hat{C}_k(L)|^2}{2\sigma_{Lk}^2}) \tag{3.10}$$

where,

$$\hat{C}_k(L) = \mathbf{E}[C_k(L) \,|\mathbf{m}_{kL}] \tag{3.11}$$

$\hat{C}_{kL}$ is the MMSE estimate of $C_k(L)$ given the information vector $\mathbf{m}_{kL}$ and

$$2\sigma_{Lk}^2 = \mathbf{E}[\,|C_k(L) - \hat{C}_k(L)|^2 \;|\; \mathbf{m}_{kL}] \tag{3.12}$$

is the mean squared error in estimation, conditioned upon $\mathbf{m}_{kL}$. $C_k(L)$ is a zero mean complex Gaussian random variable with variance $2\alpha_{Lk}^2 = T_p\, \Phi_c(kT_p;LT)$; where $\Phi_c(\tau;t)$ is the delay power profile of the channel. The estimate $\hat{C}_k(L)$ is also a zero mean complex Gaussian random variable with variance denoted by $2\lambda_{Lk}^2$. The error in estimation is given by:

$$e_k(L) = C_k(L) - \hat{C}_k(L) \tag{3.13}$$

$e_k(L)$ can be easily shown to be a zero mean complex Gaussian random variable with variance given by:

$$2\sigma_{Lk}^2 = 2\alpha_{Lk}^2 - 2\lambda_{Lk}^2 \tag{3.14}$$

(iii) Likelihood Ratio Test (LRT)

In formulating the LRT a Bayes strategy is considered and the performance criterion used is minimum probability of error. That is, if ϵ_L denotes the event of a decision error in the L^{th} symbol interval, it is required to minimize:

$$P(\epsilon_L) = \mathbf{E}_{\mathbf{I}_L^m}[P(\epsilon_L \,|\mathbf{I}_L^m)] \tag{3.15}$$

Minimizing (3.14) is equivalent to minimizing $P(\epsilon_L \,|\mathbf{I}_L^m)$. The

corresponding LRT is obtained as a simple extension from [23], [4] and can be written as:

$$\Lambda(L\,|\mathbf{I}_L^m) = \frac{\Lambda_1(L\,|\mathbf{I}_L^m)}{\Lambda_0(L\,|\mathbf{I}_L^m)} \underset{H(L)=H_0}{\overset{H(L)=H_1}{\gtrless}} 1 \tag{3.16}$$

where

$$\Lambda_i(L\,|\mathbf{I}_L^m) = \int P(\mathbf{R}(L)\,|H(L)=H_i, \mathbf{I}_L^m, \mathbf{C}(L))$$

$$\cdot\, P(\mathbf{C}(L)\,|H(L)=H_i, \mathbf{I}_L^m)\, d\mathbf{C}(L),\quad i=0,1 \tag{3.17}$$

Observations:

1. $\mathbf{C}(L)$ is independent of the hypothesis. Further, from (3.6)-(3.9), it is clear that, $P(\mathbf{C}(L)\,|H(L)=H_i, \mathbf{I}_L^m) = P(\mathbf{C}(L)\,|\mathbf{I}_L^m)$.
2. The hypotheses are independent of the memory information. This follows from (3.6) and (3.9).
3. $\mathbf{R}(L)$ is independent of $\mathbf{I}_L^m$. This is easily seen from (3.5). For $\mathbf{R}(L)$ given $\mathbf{C}(L)$ and the hypothesis $H(L)$, the only uncertainty in $\mathbf{R}(L)$ corresponds to the noise terms of each $r_k(L)$. These noise terms are z_{kj}^1 and z_{kj}^0, which are uncorrelated for all k and j. Hence, $\mathbf{R}(L)$ is independent of $\mathbf{I}_L^m$.

Using these observations (3.16) can be expressed as:

$$\Lambda_i(L\,|\mathbf{I}_L^m) = \int P(\mathbf{R}(L)\,|H(L)=H_i, \mathbf{C}(L))$$

$$\cdot\, P(\mathbf{C}(L)\;|\;\mathbf{I}_L^m)\, d\mathbf{C}(L),\quad i=0,1 \tag{3.18}$$

Now from (3.4) and the definition of $\mathbf{R}(L)$ it is easily seen that:

$$P(\mathbf{R}(L)\;|\;H(L)=H_i, \mathbf{C}(L)) =$$

$$\left(\frac{1}{\pi N_o}\right)^{2N_c} \prod_{k=1}^{N_c} \exp\left[-\frac{|r_k(L) - i\,A\sqrt{E_p}\,C_k(L)\,|^2}{N_o}\right] \cdot$$

$$\prod_{k=N_c+1}^{2N_c} exp\left[-\frac{|r_k(L) - (1-i)\, A\sqrt{E_p}\, C_{\overline{k-N_c}}(L)|^2}{N_o}\right] \tag{3.19}$$

where i = 0, 1. By using a binary symmetric hypothesis formulation for the problem it was not necessary to divide numerator and denominator of the LRT by the hypothesis under which only noise is received, as in [4].

Substituting (3.18) and (3.19) in (3.16) the LRT can be simplified to yield the following receiver structure:

$$\sum_{k=1}^{N_c}\left[\frac{A^2E_p\, 2\sigma_{Lk}^2}{N_o + A^2E_p\, 2\sigma_{Lk}^2}\,|r_k^1(L)|^2 + \frac{N_o}{N_o + A^2E_p\, 2\sigma_{Lk}^2}\, 2Re\{r_k^1(L)\,\hat{C}_k^*(L)\}\right]$$

$$\underset{H(L)=H_0}{\overset{H(L)=H_1}{\gtrless}}$$

$$\sum_{k=1}^{N_c}\left[\frac{A^2E_p\, 2\sigma_{Lk}^2}{N_o + A^2E_p\, 2\sigma_{Lk}^2}\,|r_k^\circ(L)|^2 + \frac{N_o}{N_o + A^2E_p\, 2\sigma_{Lk}^2}\, 2Re\{r_k^\circ(L)\,\hat{C}_k^*(L)\}\right] \tag{3.20}$$

where $r_k^1(L) = r_k(L)$ and $r_k^\circ(L) = r_{\overline{k+N_c}}(L)$

Each side of the LRT, described by (3.20), is illustrated in Figure 3.1. On each diversity branch there is a dual combination of coherent and non-coherent processing, the choice of one or the other is determined by the factor $A^2E_pN_o^{-1}\, 2\sigma_{Lk}^2$, which is determined by the average SNR on each branch. This receiver is considered to be partially coherent.

Case 2 Coherent Multipath Diversity Receiver

If the estimation process yields perfect estimates then $2\sigma_{Lk}^2 = 0$ and $\hat{C}_k(L) = C_k(L)$. The corresponding receiver structure can be deduced from (3.19) to be:

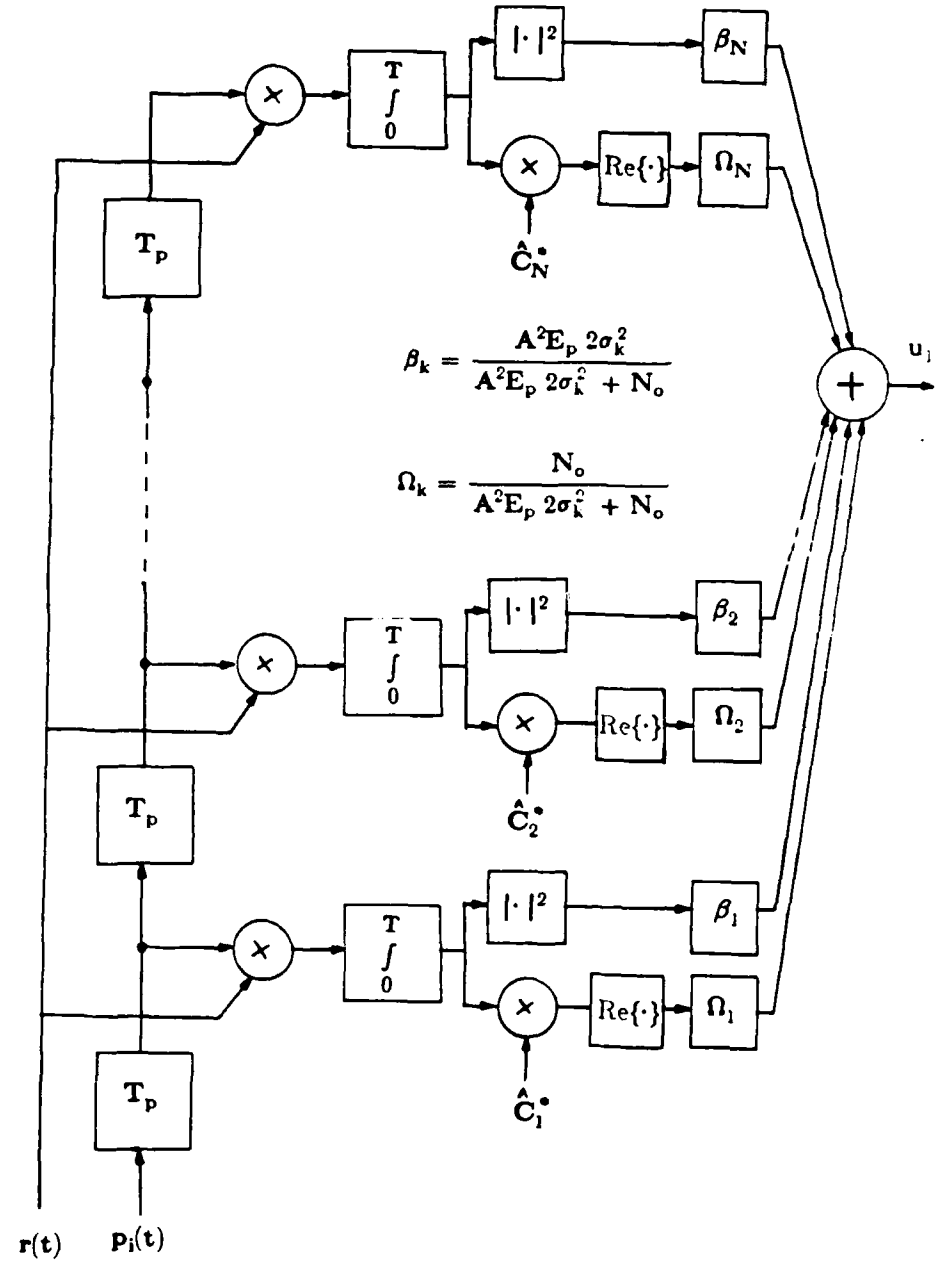

Figure 3.1 Adaptive estimator-correlator structure for orthogonal signaling.

$$\sum_{k=1}^{N_c} \mathrm{Re}\{r_k^1(L)\, C_k^*(L)\} \underset{H(L)=H_o}{\overset{H(L)=H_1}{\gtrless}} \sum_{k=1}^{N_c} \mathrm{Re}\{r_k^o(L)\, C_k^*(L)\} \tag{3.21}$$

This is similar to the ideal coherent RAKE correlator [16], [18].

Case 3 Non-Coherent Multipath Diversity Receiver

Consider the case when the estimation process yields very poor estimates. Since $2\sigma_{Lk}^2 = 2\alpha_{Lk}^2 - 2\lambda_{Lk}^2$, the maximum value of $2\sigma_{Lk}^2$ occurs when $2\lambda_{Lk}^2 = 0$. This implies no estimation or $\hat{C}_k(L) = 0$. Substituting $\hat{C}_k(L) = 0$ in (3.20) yields:

$$\sum_{k=1}^{N_c} \beta_k \left| r_k^1(L) \right|^2 \underset{H(L)=H_o}{\overset{H(L)=H_1}{\gtrless}} \sum_{k=1}^{N_c} \beta_k \left| r_k^o(L) \right|^2 \tag{3.22}$$

where

$$\beta_k = \frac{A^2 E_p\, T_p \cdot \Phi_c(kT_p;LT)}{A^2 E_p\, T_p \cdot \Phi_c(kT_p;LT) + N_o} = \frac{\lambda_k(LT)}{\lambda_k(LT) + N_o}$$

and from (3.3),

$$r_k^i(L) = \int_0^T r(t)\, p_i(t - kT_p)\, dT \quad i = 0, 1$$

$\lambda_k(LT)$ is simply the eigenvalue of the k^{th} path in the L^{th} signaling interval.

Since DSSS codes are used, the receiver structure of (3.20), (3.21) and (3.22) can be modified for easier implementation. That is, in Figure 3.1 the branch multipliers can be replaced by switches and the integrators replaced by summers. The summer-square combination may also be realized using an envelope detector, [12].

3.3 Estimation Schemes

From the receiver structure of (3.20) it is clear that for coherent processing on each branch it is necessary to estimate C_k. In this section decision directed estimation (DDE) and non-decision directed estimation (NDDE) are considered. The estimator is formulated based on the discrete Wiener-Hopf filter. Since the memory information, used

to estimate the channel coefficients C_k, can be partitioned into independent blocks, one for each channel coefficient, the estimator need be formulated only for a single path. All other branches of the receiver will employ identical estimators.

From (3.5)-(3.7) it is clear that the estimation problem comprises estimating a Gaussian parameter in AWGN. The memory information from which the estimate is derived is also Gaussian. For this Gaussian estimation problem the optimal MMSE estimator is linear and of the form, [1]:

$$\hat{C}_k(L) = \sum_{j=L-M_b}^{L-1} W_{kj}\, V_k(j) \tag{3.23}$$

where $V_k(j)$ is determined from (3.6) and (3.7).

The weights $\{W_{kj}\ ,\ j = (L - M_b),\ \cdots,\ (L-1)\}$ are chosen to make $\hat{C}_k(L)$ a MMSE estimate. The optimal weights can be shown, from the orthogonality principle, to be a solution of M_b discrete Wiener-Hopf equations, [1], given by:

$$\phi_{C_k}(L-i) = \sum_{j=L-M_b}^{L-1} W_{kj}[A\sqrt{E_p}\ \phi_{C_k}(j-i) + hN_o\ \delta(j-i)]\ ,$$

$$i = (L - M_b),\ \cdots,\ (L-2),\ (L-1) \tag{3.24a}$$

where,

$$\phi_{C_k}(j-i) \triangleq E[C_k(j)\ C_k^*(i)] = T_p\ \Phi_c(kT_p;\overline{j-i}T) \tag{3.24b}$$

and h=1 for DDE and h=2 for NDDE.

The mean square error in estimation can be determined, as in [14], to be:

$$2\sigma_{Lk}^2 = \phi_{C_k}(0) - A\sqrt{E_p} \sum_{j=L-M_b}^{L-1} W_{kj}\ \phi_{C_k}(L-j) \tag{3.25}$$

For a quasi-static channel the solution to (3.24a) can be obtained, for

any M_b, using the Sherman Morrison Inverse matrix identity, [11]. The solution for the optimal weights can be shown to be:

$$W_{k1} = W_{k2} = \cdots = W_{kM_b} = W_k = \frac{A\sqrt{E_p}\,\phi_{C_k}(0)}{A^2E_p\phi_{C_k}(0)\,M_b + hN_o} \tag{3.26}$$

From (3.25) and (3.26) the mean square error is:

$$2\sigma_{Lk}^2 = \frac{\phi_{C_k}(0)\,hN_o}{A^2E_p\,\phi_{C_k}(0)\,M_b + hN_o} \tag{3.27}$$

When $A^2E_p\,\phi_{c_k}(0)\,M_b \gg hN_o$, which occurs when M_b is large and the average SNR per path is high, then (3.26) and (3.27) reduce to:

$$W_k = \frac{1}{A\sqrt{E_p}\,M_b} \tag{3.28}$$

and

$$2\sigma_{Lk}^2 = \frac{1}{A^2E_p} \cdot \frac{hN_o}{M_b} \tag{3.29}$$

Hence, when the average SNR per path is high (weak fade or large M_b) (3.28) can be used in (3.23) to give:

$$\hat{C}_k(L) = \frac{1}{A\sqrt{E_p}\,M_b} \sum_{j=L-M_b}^{L-1} V_k(j) \tag{3.30}$$

Thus, from (3.30) it is seen that the estimate is derived by averaging the memory information over M_b symbol intervals. This process is equivalent to filtering the memory information using a band-pass filter with bandwidth greater than the fade rate.

With DDE if a bit decision is incorrect it will propagate throughout the memory length causing a string of estimation errors and hence further bit decision errors. The effect may lead to a *run-away* condition, [17], and can be ameliorated by using a short memory

or exponential weights.

The function of exponential weights, in the sample mean estimator, is to emphasize the recent bit decisions with respect to the past bit decisions. One form of these weights is:

$$W'_{kj} = 2 \left(\frac{M_b - 1}{M_b + 1} \right)^{L-j} W_{kj} \tag{3.31}$$

The use of exponential weights given by (3.31) is suggested for a practical sample mean estimator using DDE. It can be shown that by using these exponential weights, there will be a small reduction in the amplitude of the estimated path coefficient $\hat{C}_k$ and hence a small reduction in the estimated SNR per path.

3.4 Performance of Partially Coherent Receiver

3.4.1 Uniform Delay Power Profile

The receiver structure of (3.20) can be modified by adding $N_o^2(A^2E_p\,(2\sigma_{Lk}^2)^2 + N_o 2\sigma_{Lk}^2)^{-1}\ |\hat{C}_k(L)\,|^2$, $k = 1, 2, \ldots, N_c$ to both sides of the LRT. The resulting structure can be rewritten as:

$$\sum_{k=1}^{N_c} \beta_k \left[\, |X_k(L)\,|^2 - |Y_k(L)\,|^2 \right] \underset{H(L)=H_0}{\overset{H(L)=H_1}{\gtrless}} 0 \tag{3.32a}$$

where

$$\beta_k = \frac{N_o}{A^2E_p\ 2\sigma_{Lk}^2 + N_o} \cdot \left(\frac{N_o}{A^2E_p\ 2\sigma_{Lk}^2} \right) \tag{3.32b}$$

$$X_k(L) = \frac{A^2E_p\ 2\sigma_{Lk}^2}{N_o}\, r_k^1(L) + \hat{C}_k(L) \tag{3.32c}$$

$$Y_k(L) = \frac{A^2E_p\ 2\sigma_{Lk}^2}{N_o}\, r_k^0(L) + \hat{C}_k(L) \tag{3.32d}$$

For a uniform delay power profile all channels are identical and $2\alpha_{Lk}^2 = N_c^{-1}$, k=1, 2, ..., N_c. Further, from (3.27) or (3.29), $2\sigma_{Lk}^2 = 2\sigma_L^2$. Recalling that the order of diversity N_d is usually less than equal to N_c, (3.32a) can be rewritten as:

$$D(L) \triangleq \sum_{k=1}^{N_d} |X_k(L)|^2 - |Y_k(L)|^2 \underset{H(L)=H_o}{\overset{H(L)=H_1}{\gtrless}} 0 \tag{3.33}$$

The probability of error is given by:

$$P(e) = P(D(L) < 0 \mid H(L) = H_1)\, P(H(L) = H_1)$$

$$+ P(D(L) > 0 \mid H(L) = H_0)\, P(H(L) = H_0) \tag{3.34}$$

For a binary symmetric hypothesis problem with equally likely hypothesis, (3.34) reduces to:

$$P(e) = P(D(L) < 0 \mid H(L) = H_1) \tag{3.35}$$

To determine P(e), first the conditional error probability $P(e \mid \mathbf{I}_L^m)$ is determined. This is of the form:

$$P(e \mid \mathbf{I}_L^m) = P(D(L) < 0 \mid H(L) = H_1, \mathbf{I}_L^m) \tag{3.36}$$

To evaluate (3.37) one needs to know the statistics of $\{X_k(L) \mid H(L) = H_1, \mathbf{I}_L^m\}$ and $\{Y_k(L) \mid H(L) = H_1, \mathbf{I}_L^m\}$. From (3.5), (3.32c) and (3.32d) it can be shown that $\{X_k(L) \mid H(L) = H_1, \mathbf{I}_L^m\}$, k = 1, 2, ..., N_c are i.i.d. complex Gaussian random variables with mean μ_{X_k} and variance σ_X^2, where:

$$\mu_{X_k} = (1 + A\sqrt{E_p}\gamma_L)\, \hat{C}_k(L) \tag{3.37a}$$

$$\sigma_X^2 = \gamma_L^2(A^2 E_p\, 2\sigma_L^2 + N_o) \tag{3.37b}$$

where

$$\gamma_L = \frac{A^2 E_p \, 2\sigma_L^2}{N_o}$$

Similarly, $\{Y_k(L) \mid H(L) = H_1, I_L^m\}$, $k = 1, 2, ..., N_d$, are i.i.d. complex Gaussian random variables with mean μ_{Y_k} and variance σ_Y^2, given by:

$$\mu_{Y_k} = \hat{C}_k(L) \tag{3.37c}$$

$$\sigma_Y^2 = \gamma_L^2 \, N_o \tag{3.37d}$$

Also, the covariance, between the two conditional variables, can be shown to be:

$$\mu_{X_k Y_k} = 0, \quad k = 1, 2, ..., N_d \tag{3.37e}$$

The general quadratic form of a decision variable is given by:

$$D = \sum_{k=1}^{N} [A \, |X_k|^2 + B \, |Y_k|^2 + C \, X_k Y_k^* + C^* X_k^* Y_k] \tag{3.38}$$

where A, B, C are constants, $\{X_k, Y_k\}$ are a pair of correlated complex Gaussian random variables and the N pairs $\{X_k, Y_k\}$ are mutually statistically independent and identically distributed.

For the general quadratic form of (3.38) a probability of error expression has been derived in Appendix 4B of [18]. From (3.33) and (3.38) it is clear that $\{D(L) \,|H(L) = H_1, I_L^m\}$ is a quadratic form in complex Gaussian random variables with $A = 1$, $B = -1$ and $C = 0$. Applying the results of Appendix 4B of [17], the conditional probability of error for (3.36) can be expressed as:

$$P(e_L \,|I_L^m) = Q[\sqrt{k_3 x_L}, \sqrt{k_4 x_L}]$$

$$+ [A(N_d) - 1] \, I_o(\beta \, x_L) \exp\left(-\frac{k_3 + k_4}{2} \, x_L\right)$$

$$+ \sum_{n=1}^{N_d} B(n, N_d)\, I_n(\beta x_L) \exp\left[-\frac{k_3 + k_4}{2} x_L\right] \tag{3.39}$$

where

$$k_3 = \frac{2}{N_o(2+\gamma_L)\gamma_L^2} \;,\; k_4 = (A^2 E_p \gamma_L + 1)^2 k_3$$

$$\beta = \sqrt{k_3 k_4} \;,\; \chi = \frac{k_3 + k_4}{2} + \frac{1}{2\lambda_L^2} \;,\; x_L = \sum_{k=1}^{N_d} |\hat{C}_k(L)|^2$$

$$A(N_d) = \sum_{k=0}^{N_d-1} \binom{2N_d-1}{k} \frac{(1+\gamma_L)^k}{(2+\gamma_L)^{2N_d-1}}$$

$$B(n,N_d) = \sum_{k=0}^{N_d-n-1} \binom{2N_d-1}{k} \left[\frac{(1+\gamma_L)^k (1+A\sqrt{E_p}\gamma_L)^n}{(2+\gamma_L)^{2N_d-1}}\right]$$

$$- \left[\frac{(1+\gamma_L)^{2N_d-1-k} (1+A\sqrt{E_p}\gamma_L)^{-n}}{(2+\gamma_L)^{2N_d-1}}\right]$$

Further, $I_n(\cdot)$ is the n^{th} order modified Bessel function of the first kind and Q(a,b) is the Q-function as defined in [22].

The probability of error can be determined by averaging (3.39) with respect to the p.d.f of x_L. Given the memory information I_L^m, x_L is known. Hence, the probability of error is given by:

$$P(e) = \int_0^\infty P(e\,|I_L^m)\, P(x_L)\, dx_L \tag{3.40}$$

For a uniform delay power profile $\hat{C}_k(L)$ are a set of i.i.d. zero mean complex Gaussian random variables with variance

$2\lambda_{Lk}^2 = 2\lambda_l^2$, $k = 1, 2, \ldots, N_c$.

Therefore, x_L has a gamma p.d.f. given by:

$$P(x_L) = \frac{1}{(N_d-1)!} \frac{x_L^{N_d-1}}{(2\lambda_L^2)^{N_d}} \exp\left(-\frac{x_L}{2\lambda_L^2}\right) \quad x_L \geq 0 \tag{3.41}$$

Using (3.39) and (3.41) in (3.40) and performing the integration yields:

$$P(e) = \frac{1}{(N_d-1)!\,(2\lambda_L^2)^{N_d}} I(N_d) + [A(N_d) - 1] \left(\frac{1}{\chi \cdot 2\lambda_L^2}\right)^{N_d}$$

$$\cdot \left(1 - \frac{\beta^2}{\chi^2}\right)^{\frac{1}{2} - N_d} {}_2F_1\left(\frac{1-N_d}{2}, 1 + \frac{-N_d}{2}; 1; \frac{\beta^2}{\chi^2}\right)$$

$$+ \sum_{n=1}^{N_d-1} \left\{ B(n,N_d) \binom{N_d+n-1}{n} \left(\frac{\beta}{2\chi}\right)^n \right.$$

$$\left. \cdot {}_2F_1\left(\frac{n+1-N_d}{2}, 1 + \frac{n-N_d}{2}; n+1; \frac{\beta^2}{\chi^2}\right) \right. \tag{3.42}$$

where ${}_2F_1(a; b; c; z)$ is the Gauss Hypergeometric function and

$$I(N_d) = \int_0^\infty Q(\sqrt{k_3 x_L}, \sqrt{k_4 x_L})\, x_L^{N_d-1} \exp\left(-\frac{x_L}{2\lambda_L^2}\right) dx_L \tag{3.43}$$

It is difficult to obtain a closed form expression for (3.43) except in the form of an infinite series. The infinite series form is given by

$$I(N_d) = \sum_{j=0}^{\infty} \left(\frac{k_3}{k_4}\right)^{j/2} \left(\frac{\beta}{2\chi}\right)^j \frac{(N_d + j - 1)!}{j!} \left(1 - \frac{\beta^2}{\chi^2}\right)^{\frac{1}{2} - N_d}$$

$$\left(\frac{1}{\chi}\right)^{N_d} {}_2F_1\left(\frac{j+1-N_d}{2}, 1+\frac{j-N_d}{2}; j+1; \frac{\beta^2}{\chi^2}\right) \tag{3.44}$$

Using Parl's algorithm, [15], to compute Q(a,b), (3.54) can be conveniently evaluated by numerical integration using the NAG (Numerical Algorithm Group) routine D01AMF.

3.4.2 Non-Uniform Delay Power Profile

For a non-uniform delay power profile the average SNR on each path is different. In this section, a probability of error expression is developed for a quasi-static channel. For a quasi-static channel and the estimator of (3.30) the estimation error variance is given by, (3.29):

$$2\sigma_{Lk}^2 = 2\sigma_L^2 = \frac{hN_o}{A^2E_pM_b} \tag{3.45}$$

Following the procedure outlined for a uniform delay power profile, the conditional error probability $P(e \mid \mathbf{I}_L^m)$ is once again given by (3.39). However, for a non-uniform delay power profile the p.d.f of x_L given by:

$$P(x_L) = \sum_{k=1}^{N_d} \frac{\pi_{Lk}}{2\lambda_{Lk}^2} \exp\left(-\frac{x_L}{2\lambda_{Lk}^2}\right) \qquad x_L \geq 0 \tag{3.46}$$

where

$$\pi_{Lk} = \prod_{\substack{i=1 \\ i\neq k}}^{N_d} \frac{2\lambda_{Lk}^2}{2\lambda_{Lk}^2 - 2\lambda_{Li}^2}$$

Substituting (3.39) and (3.46) in (3.40) and solving the integral, yields:

$$P(e) = \sum_{k=1}^{N_d} \frac{\pi_{Lk}}{2\lambda_{Lk}^2} \left[I_1(N_d) + \frac{A(N_d) - 1}{\sqrt{\chi^2 - \beta^2}} \right.$$

$$+ \sum_{n=1}^{N_d-1} \frac{B(n,N_d)\,\beta^n}{\sqrt{\chi^2-\beta^2}\,[\chi+\sqrt{\chi^2-\beta^2}]^n} \tag{3.46}$$

where, $\chi = (k_3 + k_4)/2 + (\lambda_{Lk}^2)^{-1}$. k_3, k_4, $A(N_d)$, $B(n,N_d)$, β are as defined in (3.39) and

$$I_1(N_d) = \int_0^\infty Q(\sqrt{k_3 x_L}, \sqrt{k_4 x_L}) \exp\left(-\frac{x_L}{2\lambda_{Lk}^2}\right) dx_L \tag{3.47}$$

A useful computational form of (3.47) can be obtained by expressing it in an infinite series form given by:

$$I_1(N_d) = \sum_{j=0}^{\infty} \left(\frac{k_3}{k_4}\right)^{j/2} \frac{\beta^j}{\sqrt{\chi^2-\beta^2}[\chi+\sqrt{\chi^2-\beta^2}]^j} \tag{3.48}$$

This is a convergent series which can be evaluated accurately and rapidly, using the NAG library routine CO6BAF, using a 50 term approximation.

All the probability of error expressions derived in this section hold only for $2\alpha_{Lk}^2 > 2\lambda_{Lk}^2$. This is reasonable since if the reverse were true it would imply that the error variance were negative.

3.5 Approximations and Bounds

This section discusses upper and lower bounds on the probability of error, as a function of the knowledge of channel states. This knowledge of channel states is expressed in the definition:

$$\rho_k = \frac{\mathbf{E}[C_k(L)\,\hat{C}_k^*(L)]}{[\mathrm{Var}\{C_k(L)\}\,\mathrm{Var}\{\hat{C}_k(L)\}]^{1/2}} \tag{3.49}$$

where $k = 1, 2, \ldots, N_d$. ρ_k expresses the degree of correlation between $C_k(L)$ and $\hat{C}_k(L)$. Further, (3.49) can be simplified and expressed as:

$$\rho_k = \left(\frac{2\lambda_{Lk}^2}{2\alpha_{Lk}^2} \right)^{1/2} \tag{3.50}$$

3.5.1 Lower Bound

When $\rho_k = 1$, it follows from (3.14) and (3.50) that $2\sigma_{Lk}^2 = 0$. This implies that $\hat{C}_k(L) = C_k(L)$, indicating perfect estimation. When this condition is satisfied for all k branches, then as in (3.21) perfectly coherent detection is possible and the corresponding error probability will be a lower bound.

From the estimator structure of (4.40), $2\sigma_{Lk}^2 \rightarrow 0$ for all k branches when the average SNR per path is high (M_b fixed, $N_o \ll 1$). Under this high SNR condition the following approximations, with regard to (3.42) hold:

High SNR Approximations:

As $2\sigma_{Lk}^2 \rightarrow 0$, $\gamma_L \rightarrow 0$, $B(n, N_d) \rightarrow 0$, $\chi \gg 1$, $(\frac{1}{\chi})^{N_d} \rightarrow 0$, and $2\lambda_L^2 \rightarrow 2\alpha_L^2$.
Using these approximations, (3.42) can be reduced to:

$$P(e) \simeq$$

$$\frac{1}{(N_d-1)!\, 2\alpha_L^2} \int_0^\infty Q(\sqrt{k_3 x_L}, \sqrt{k_4 x_L})\, x_L^{N_d-1} \exp\left(- \frac{x_L}{2\alpha_L^2} \right) dx_L \tag{3.51}$$

Now as $\gamma_L \rightarrow 0$, $k_3 \gg 1$, $k_4 \gg 1$ and $k_4 \rightarrow k_3$. Also, $k_4 \gg k_4 - k_3$. Under these conditions the following approximation is valid, [22]:

$$Q(\sqrt{k_3 x_L}, \sqrt{k_4 x_L}) \simeq \frac{1}{2} \operatorname{erfc}\left[\frac{(\sqrt{k_4} - \sqrt{k_3})\sqrt{x_L}}{\sqrt{2}} \right]$$

$$= \frac{1}{2} \operatorname{erfc}\left(\frac{A^2 E_p x_L}{2\, N_o} \right)^{1/2} \tag{3.52}$$

Substituting (3.52) in (3.51) and integrating by parts, yields:

$$P(e) \simeq \frac{1}{2}\left[1 - \mu_1 \sum_{k=0}^{N_d-1} \binom{2k}{k} \left(\frac{1-\mu_1^2}{4}\right)^k\right] \tag{3.53}$$

where

$$\mu_1 = \left(\frac{\bar{\gamma}_c}{\bar{\gamma}_c + 2}\right)^{1/2} \quad ; \quad \bar{\gamma}_c = \frac{A^2 E_p \, 2\alpha_L^2}{N_o}$$

Similarly, for a non-uniform delay power profile the lower bound on the probability of error can be obtained by making the same high SNR approximations. These approximations allow (3.46) to be expressed as:

$$P(e) \simeq \sum_{k=1}^{N_d} \frac{\pi_{Lk}}{2\lambda_{Lk}^2}\left[\int_0^\infty \frac{1}{2}\,\mathrm{erfc}\left(\frac{A^2 E_p x_L}{2N_o}\right)^{1/2} \exp\left(-\frac{x_L}{2\lambda_{Lk}^2}\right) dx_L\right] \tag{3.54}$$

Integrating (3.54) by parts and simplifying yields:

$$P(e) \simeq \frac{1}{2}\sum_{k=1}^{N_d} \pi_{Lk}\left[1 - \left(\frac{A^2 E_p \, 2\alpha_{Lk}^2}{A^2 E_p \, 2\alpha_{Lk}^2 + 2N_o}\right)^{1/2}\right] \tag{3.55}$$

Equations (3.52) and (3.55) only hold for high SNR and are similar to the probability of error expressions obtained for a perfectly coherent RAKE receiver, [18].

3.5.2 Upper Bound

When $\rho_k \rightarrow 0$, the estimate $\hat{C}_k(L)$ is totally decorrelated from $C_k(L)$ and no useful estimate can be obtained. This condition typically occurs when the channel fades rapidly, as in a mobile radio channel. This implies that the estimator cannot track the channel coefficients. With regard to the estimator of (3.40), this means that the fade rate is much higher than the estimator filter bandwidth and hence no sample mean estimate can be obtained. Under this condition,

non-coherent detection is done. Although $\rho_k \rightarrow 0$ can occur for low and high SNR our interest is in the high SNR case as this represents the worst case and hence the corresponding error probability will be upper bound on performance.

Equation (3.42) can be rewritten, using (3.44), as:

$$P(e) = \left(\frac{1}{\chi\, 2\lambda_L^2}\right)^{N_d} \left[[A(N_d) - 1]\ {}_2F_1\left(\frac{1-N_d}{2}, 1-\frac{N_d}{2}; 1; \frac{\beta^2}{\chi^2}\right)\right.$$

$$+ \sum_{n=1}^{N_d-1} \binom{N_d + n-1}{n} \left(\frac{\beta}{2\chi}\right)^n \left[B(n, N_d) + \left(\frac{k_3}{k_4}\right)^{n/2}\right]$$

$${}_2F_1\left(\frac{n+1-N_d}{2}, 1 + \frac{n-N_d}{2}; n+1; \frac{\beta^2}{\chi^2}\right)$$

$$+ \sum_{n=N_d}^{\infty} \binom{N_d + n - 1}{n} \left(\frac{\beta}{2\chi}\right)^n \left(\frac{k_3}{k_4}\right)^{n/2}$$

$$\left.{}_2F_1\left(\frac{n+1-N_d}{2}, 1 + \frac{n-N_d}{2}; n+1; \frac{\beta^2}{\chi^2}\right)\right] \qquad (3.56)$$

For high SNR, corresponding to $P(e) \geq 10^{-3}$, if $\rho_k \rightarrow 0$ for $k=1, 2, \ldots, N_d$, then $2\lambda_{Lk}^2 \rightarrow 0$ and $2\alpha_{Lk}^2 = 2\sigma_{Lk}^2$ for $k=1,2,\ldots N_d$. Further, $\chi \gg 1$, $\chi \gg \beta$ and $k_3 \ll k_4$.

Applying these high SNR approximations to (3.56) yields:

$$P(e) \simeq \left(\frac{1}{\chi\, 2\lambda_L^2}\right)^{N_d} \left[1 - \frac{\beta^2}{\chi^2}\right]^{\frac{1}{2} - N_d} \left[A(N_d) - 1\right] \left(\frac{\beta}{2\chi}\right)^n$$

$$+ \sum_{n=1}^{N_d-1} \binom{N_d + n - 1}{n} \left(\frac{\beta}{2\chi}\right)^n \left[B(n,N_d) + \left(\frac{k_3}{k_4}\right)^{n/2}\right] \qquad (3.57)$$

Equation (3.57) is found to be an excellent approximation to the error

probability of a Square-Law receiver. This is an upper bound which also holds for a non-uniform profile due to the following reason. As $\rho_k \rightarrow 0$, $2\lambda_{Lk}^2 \rightarrow 0$ and hence $2\alpha_{Lk}^2 = 2\sigma_{Lk}^2 = hN_o(A^2E_pM_b)^{-1}$, for all k branches. Hence, this case reduces to that of a uniform delay power profile, since all paths now exhibit equal average SNR.

This result provides an interesting interpretation. When the estimate is completely decorrelated from the actual channel coefficient there is no knowledge of the path gain. Therefore, the receiver *assumes* identical paths, even though the profile may be non-uniform, and performs Square-Law detection. Since the Square-Law receiver provides an upper bound on performance, this action of the receiver may be viewed as a *minimax* operation.

3.6 Performance Evaluation for Orthogonal Signaling

The performance of the partially coherent receiver is evaluated for an illustrative indoor channel exhibiting an RMS multipath spread of 250 ns. A data rate of 32 kbps and a code length of 255 chips were assumed. Figures 3.2 and 3.3 illustrate the improvement in performance with higher orders of diversity. Figures 3.2 and 3.3 also indicate the superiority of DDE over NDDE. The improvement for DDE is due to 3 dB lower noise power in its phase estimation process. It has been assumed that the DDE scheme is ideal. However, in practice, DDE cannot be used at low SNR due to decision errors. NDDE can be used at low SNR and the receiver can switch to DDE at a higher SNR or when there is a low error rate. The switch can be done by monitoring the error rate from pilot information placed in message headers.

It is also observed from Figure 3.2 that the improvement for DDE over NDDE increases with diversity order. This is because as the number of diversity branches increase, so does the excess noise due to NDDE.

Figure 3.4 compares the use of the sub-optimal sample mean estimator versus the Wiener-Hopf estimator of Section 3.3.1. The comparison was for a uniform delay power profile, DDE and $M_b = 10$. It is seen that over the range of practical error rates ($P(e) \leq 10^{-3}$) the more practical sub-optimal estimator performs as well as the Wiener-Hopf estimator. At low SNR the improvement obtained from the Wiener-Hopf estimator is only observed for higher orders of diversity. At low values of SNR, to achieve the same performance as the optimal Wiener-Hopf estimator, the sample mean estimator must use a larger memory length.

Figure 3.5 illustrates the effect of increasing the memory length of the estimator. It is observed that for a channel with uniform delay power profile as $M_b \rightarrow \infty$ the probability of error approaches the lower bound, due to perfectly coherent reception. It is observed that

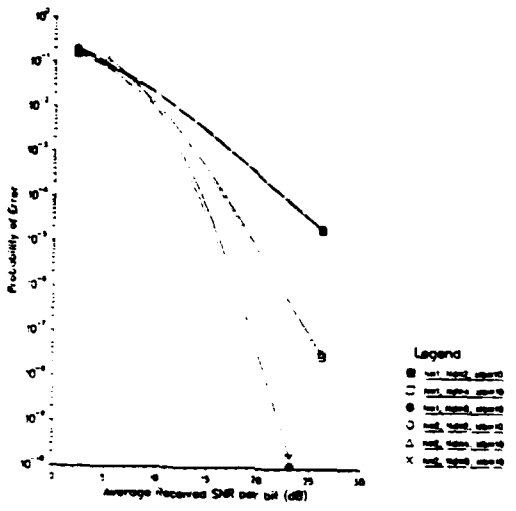

Figure 3.2 Probability of error for DDE and NDDE - Uniform delay power profile.

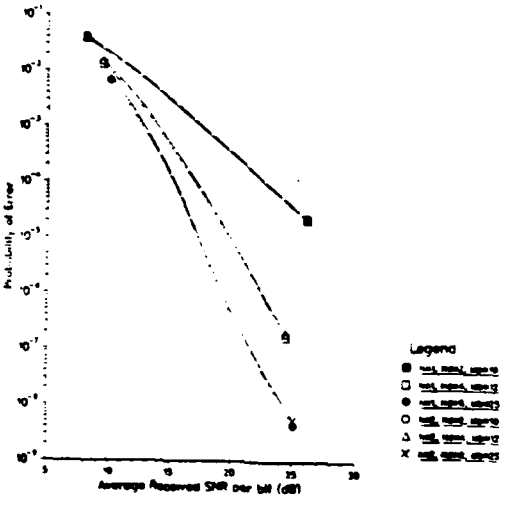

Figure 3.3 Probability of error for DDE and NDDE - Exponential delay power profile.

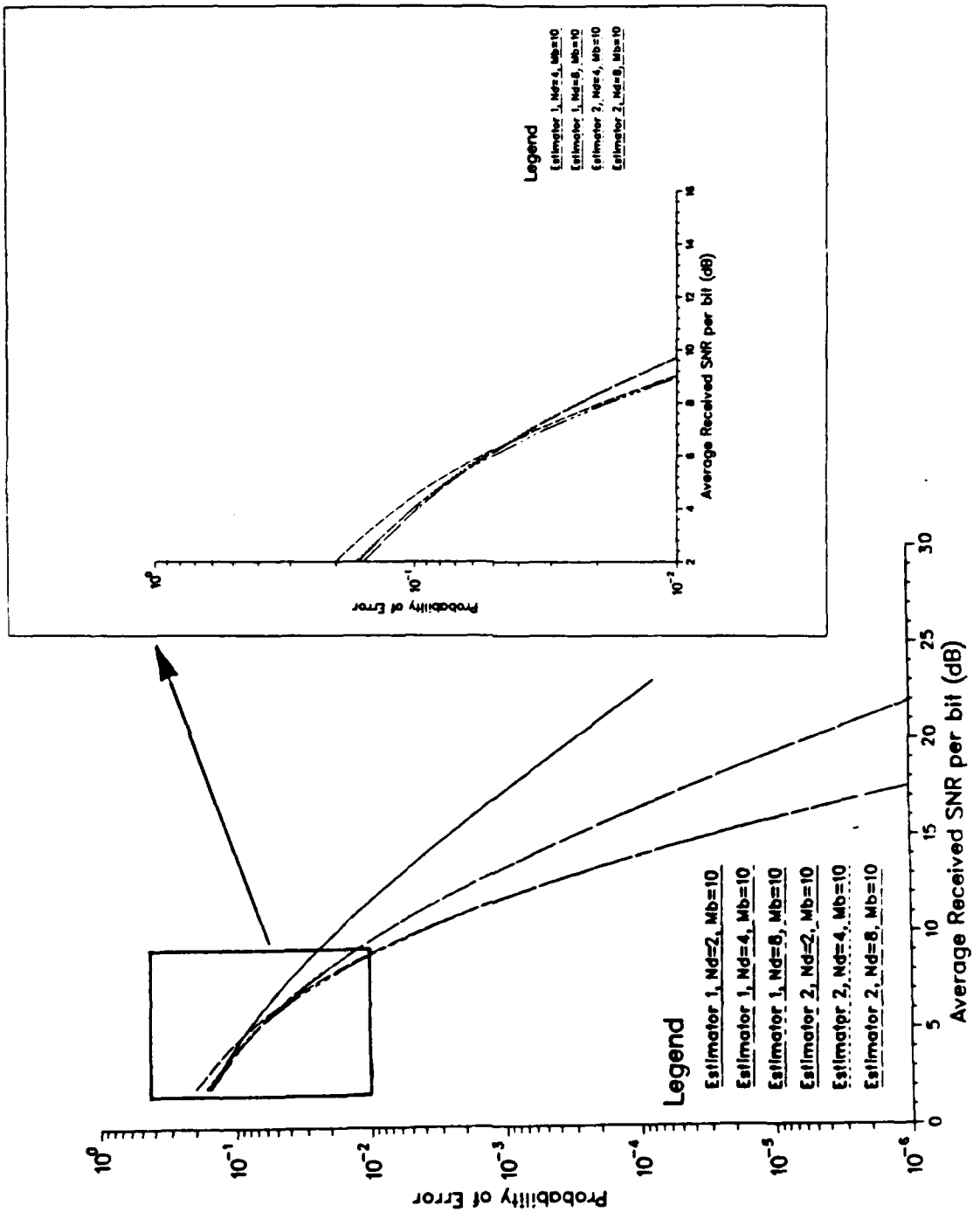

Figure 3.4 Probability of error for optimal and sub-optimal Wiener filtering schemes - Uniform delay power profile.

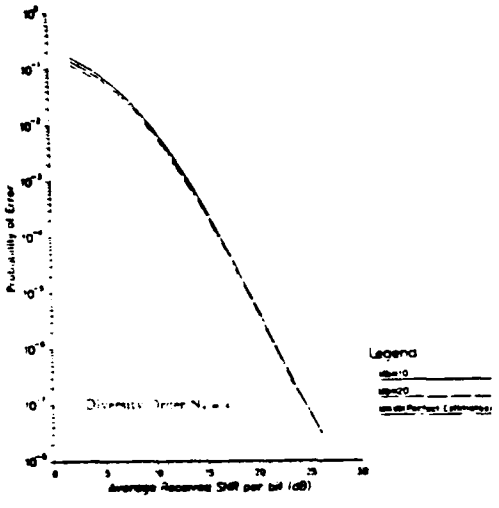

Figure 3.5 Probability of error for increasing lengths of estimator memory - Uniform delay power profile.

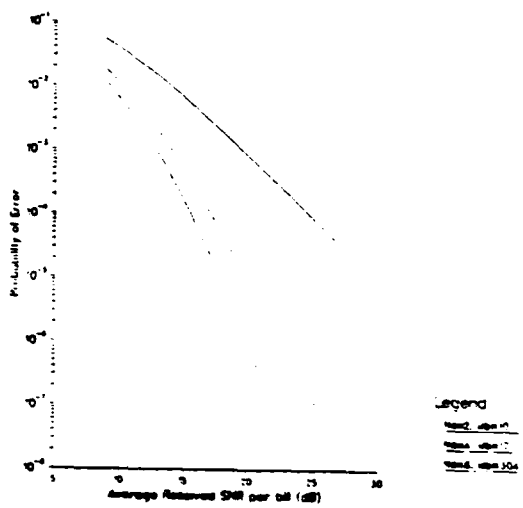

Figure 3.6 Effect of diversity order on memory length - Gaussian delay power profile

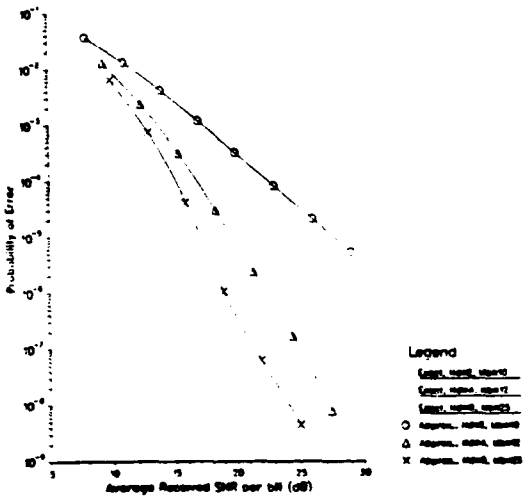

Figure 3.7 Comparison of approximation and exact expressions for probability of error of partially coherent receiver - Exponential delay power profile.

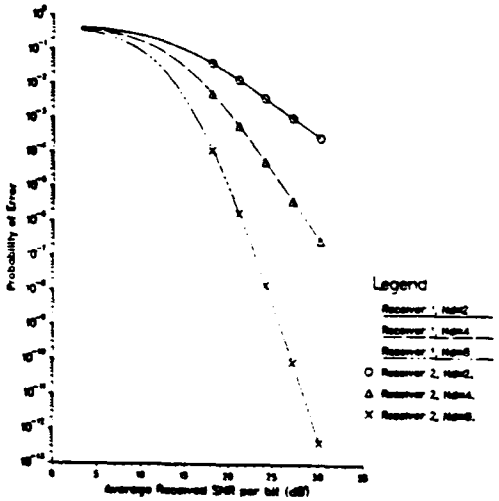

Figure 3.8 Effect of decorrelated estimates on probability of error - Uniform delay power profile.

for $M_b = 10$ the degradation in performance, for $P(e) < 10^{-3}$, is less than 0.5 dB. Short memory lengths are preferred to present run-away errors.

Figure 3.5 and Figure 3.7 illustrate that although an increase in order of diversity improves performance, it is necessary to increase the memory length simultaneously. A useful interpretation relating increasing memory length and diversity order is obtained as follows. It is desirable to choose the memory length of the sample mean estimator so that it has the same error variance as the Wiener-Hopf estimator.

Equating (3.27) and (3.29) gives:

$$\frac{T_p\,\Phi_c(kT_p)\,hN_o}{A^2E_p\,T_p\,\Phi_c(kT_p)\,M_b + hN_o} = \frac{hN_o}{A^2E_p\,M_b^1} \tag{3.58}$$

where M_b^1 is the memory length of the sample mean estimator that is required to obtain the same error variance as the optimal Wiener-Hopf estimator, with memory length M_b. Now (3.58) can be rewritten as:

$$M_b^1 = M_b + \frac{hN_o}{T_p\,\Phi_c(kT_p)} \tag{3.59}$$

Hence, for a fixed error rate (fixed N_o) and fixed code rate (T_p), M_b^1 depends inversely on the average path strength, $\Phi_c(kT_p)$. For large orders of diversity, the inclusion of weak paths cause M_b^1 to get very large. This increase in memory length should not exceed the channel coherence time (T_c), since if $M_bT > T_c$ then the estimator filter will have a bandwidth smaller than the fade rate and decorrelated estimates will be obtained followed by performance degradation. This consideration may then dictate lower orders of diversity, so as to avoid including weak paths. Figure 3.7 also illustrates the tightness of the approximation given by (3.46) and (3.48), and hence its utility in evaluating the error probability of a partial coherent receiver for a non-uniform profile.

Figure 3.8 compares the upper bound using the high SNR approximation and decorrelated estimates, for $\rho_k = 10^{-6}\ (\simeq 0)$, with the non-coherent receiver performance. The agreement between the two curves indicate that when the channel conditions preclude estimation, it is not possible to do better than non-coherent detection.

3.7 Receiver Structures for Polyphase Signaling

The received signal, in the symbol interval $(L-1)T \leq t \leq LT$, under the two hypotheses (H_i, i = 0,1) is given by:

$$H_i = H(L)$$

$$r(t) = \sum_{k=1}^{N_c} C_k(L)\, A\, e^{j\theta_k(L)}\, p(t - kT_p) + Z(t) \tag{3.60}$$

where $\theta_i(L) = \frac{2\pi}{M}(i-1)$, i = 0, 1. p(t) is the DSSS code and Z(t) is the AWGN process with psd of N_o.

The receiver structure is derived as in Section 3.2. The receiver structure that decides between the two hypotheses (H_1, H_0) in the signaling interval $(L-1)T \leq t \leq LT$ can be shown to be:

$$\sum_{k=1}^{N_c} \frac{N_o}{A^2 E_p\, 2\sigma_{Lk}^2 + N_o}\, \mathrm{Re}[r_k(L)\, \hat{C}_k^*(L)] \underset{H(L)=H_0}{\overset{H(L)=H_1}{\gtrless}} 0 \tag{3.61}$$

where

$$r_k(L) = \int_{(L-1)T}^{LT} r_k(t)\, \frac{1}{\sqrt{E_p}}\, p(t_1 - kT_p)\, dt \quad ; \quad t_1 = t - (L-1)T \tag{3.62}$$

$\hat{C}_k(L)$ and $2\sigma_{Lk}^2$ are defined by (3.11) and (3.12). As in Section 3.2 the estimate $\hat{C}_k(L)$ is based on the memory information $\mathbf{m}_{kL} = [V_k(L-M_b) \cdots V_k(L-1)]^T$, where $V_k(j)$ is given by:

$$V_k(j) = d_j\, r_k(j) \tag{3.63}$$

d_j, is the bit decision in the j^{th} signaling interval. d_j=1 when H_1 is true and d_j=0 when H_o is true. As before, the total memory information is given by:

$$\mathbf{I}_L^m = [\mathbf{m}_{1L}\, \mathbf{m}_{2L} \cdots \mathbf{m}_{N_cL}] \tag{3.64}$$

where $\mathbf{m}_{1L}$, $\mathbf{m}_{2L} \cdots \mathbf{m}_{N_cL}$ are independent blocks of Gaussian memory information, each block being used to estimate one path coefficient.

From (3.72) and (3.73) the receiver structure can be interpreted as an adaptive estimator-correlator that provides diversity through Maximal Ratio Combining, (MRC). The structure of the receiver is shown

in Figure 3.9 and Figure 3.10.

1. Maximal Ratio Combiner (MRC)

Assuming that the sample mean estimator is used, substituting (3.29) and (3.30) in (3.61) yields:

$$\sum_{k=1}^{N_d} \mathrm{Re}\left[\sum_{j=L-M_b}^{L-1} d_j\, r_k(L)\, r_k^*(j)\right] \underset{H(L)=H_1}{\overset{H(L)=H_0}{\gtrless}} 0 \qquad (3.66)$$

where $N_d \leq N_c$, is the order of diversity employed. In practice N_d is usually chosen to be less than the total number of resolved paths, for implementation reasons.

2. Differential Detection

A differential detector can be obtained from (3.66) by using a one bit memory. For $M_b=1$ (3.66) reduces to:

$$\sum_{k=1}^{N_d} \mathrm{Re}[r_k(L)\, r_k^*(L-1)] \underset{H(L)=H_0}{\overset{H(L)=H_1}{\gtrless}} 0 \qquad (3.67)$$

This differential detector is used when Differential Phase Shift Keying (DPSK) is the source modulation.

3. M-ary Detection

For binary phase coded signaling the receiver structure, shown in Figure 3.9, can be considered to be obtained by replacing the conventional matched filter/correlator in the narrowband system with structure of (3.62). Similarly, for M-ary phase coded signaling, the receiver structure can be obtained from its narrowband analog by replacing the matched filters by the structure given in Figure 3.10. The structure of this M-phase detector is illustrated in Figure 3.11.

3.8 Performance of Coherent Receiver

Proakis, [19], has obtained probability of error expressions for adaptive reception of M-phase signals considering diversity. The derivation, therein, is fairly complex. Further, the case of a non-uniform delay power profile has not been considered.

3.8.1 Uniform Delay Power Profile

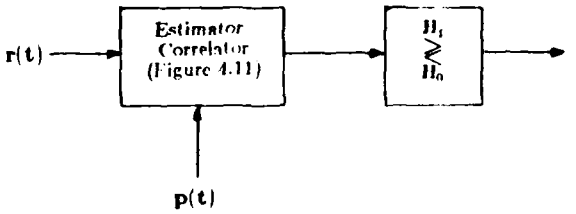

Figure 3.9 Receiver structure for BPSK signaling.

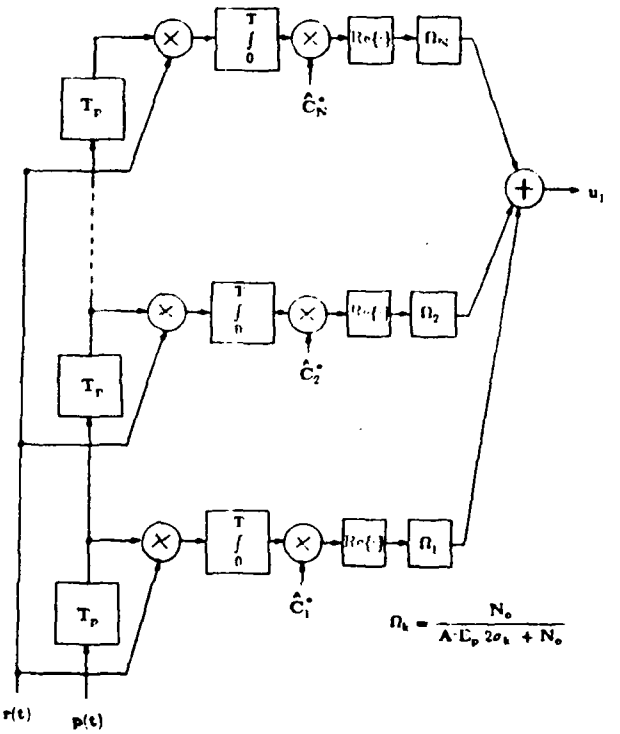

Figure 3.10 Estimator-correlator structure for BPSK signaling.

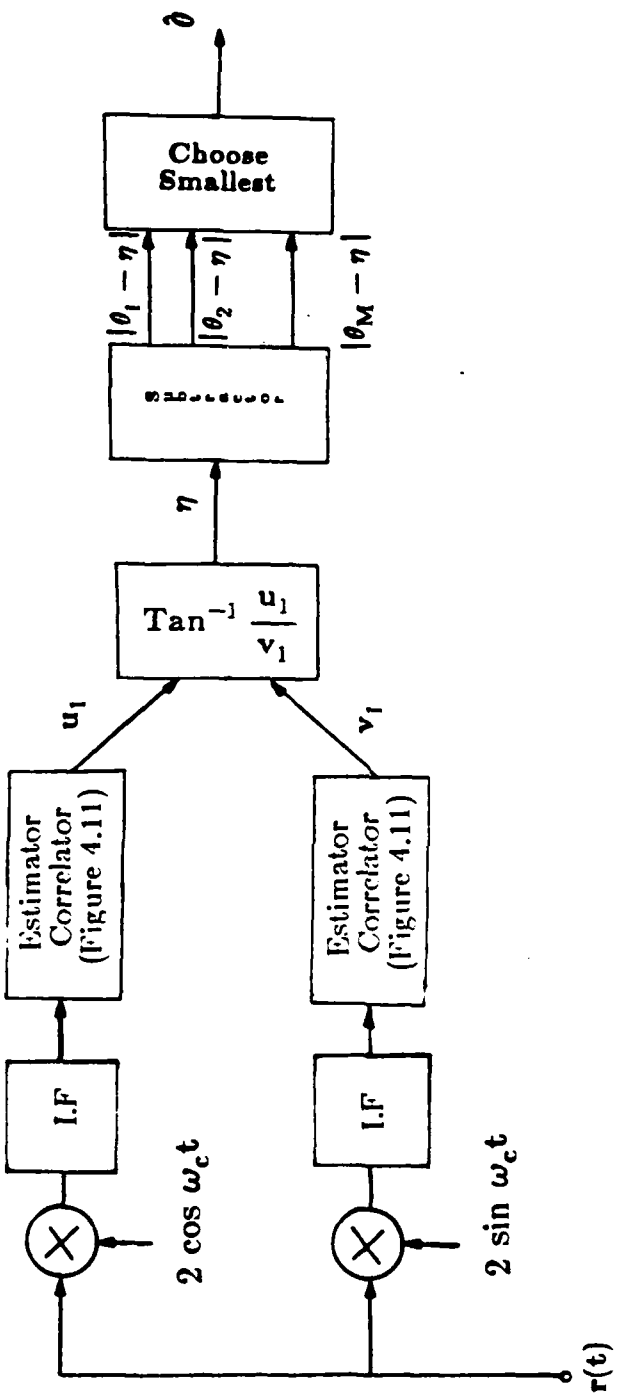

Figure 3.11 Receiver structure for Polyphase signaling.

In this case all paths are similar and $T_p \cdot \Phi_c(kT_p;0) = N_c^{-1}$ for $k = 1, 2, ..., N_c$. Hence, all paths have the same average SNR. Polyphase signaling is used and the receiver structure of Figure 3.11 is used to demodulate the received signal.

The basic decision variables $u_1(L)$, and $v_1(L)$, from Figure 3.11 and (3.66), can be written as:

$$u_1(L) = \sum_{k=1}^{N_d} \mathrm{Re}[\{A\sqrt{E_p}e^{j[\theta_i(L)]}\, C_k(L) + Z_k(L)\}\, \hat{C}_k^*(L)] \qquad (3.68a)$$

$$v_1(L) = \sum_{k=1}^{N_d} \mathrm{Re}[\{A\sqrt{E_p}e^{j[\theta_i(L)+\frac{\pi}{2}]}\, C_k(L) + Z_k(L)\}\, \hat{C}_k^*(L)] \qquad (3.68b)$$

where

$$Z_k(L) = \int_{(L-1)T}^{LT} Z(t)\, \frac{1}{\sqrt{E_p}}\, p(t_1 - kT_p)\, dt \quad ; \quad t_1 = t - (L-1)T$$

$\{Z_k(L), k = 1, 2, ..., N_d\}$ are a set of i.i.d. zero mean complex Gaussian noise random variable with variance N_o and $\theta_i(L) = 2\pi(i-1)/M$, $i = 1, 2, ..., M$.

The probability of error is derived by first determining $P(e\,|\mathbf{I}_L^m)$. If the memory information, $\mathbf{I}_L^m$, is given, it is equivalent to knowing $\{\hat{C}_k(L), k = 1, 2, \cdots N_d\}$. In order to determine $P(e\,|\mathbf{I}_L^m)$, the statistics of the decision variables $u_1(L)$ and $v_1(L)$ conditioned on $\mathbf{I}_L^m$ need to be known. It can be shown, using (3.68a) and (3.68b), that the random variables $u_1(L)$ and $v_1(L)$, conditioned on the signaling phase $\theta_i(L)$ and $\mathbf{I}_L^m$, are Gaussian with the following statistics:

$$\mathbf{E}[u_1(L)\,|\,\mathbf{I}_L^m, \theta_i(L)] = A\sqrt{E_p}\cos\theta_i(L) \sum_{k=1}^{N_d} |\hat{C}_k(L)|^2$$

$$\mathbf{E}[v_1(L)\,|\,\mathbf{I}_L^m, \theta_i(L)] = A\sqrt{E_p}\sin\theta_i(L) \sum_{k=1}^{N_d} |\hat{C}_k(L)|^2$$

$$\mathbf{Var}[u_1(L)\,|\,\mathbf{I}_L^m, \theta_i(L)] = \sum_{k=1}^{N_d} [A^2E_p\sigma_{Lk}^2 + \frac{N_o}{2}]\, |\hat{C}_k(L)|^2$$

$$\mathbf{Var}[v_1(L) \mid I_L^m, \theta_i(L)] = \sum_{k=1}^{N_d} [A^2 E_p \sigma_{Lk}^2 + \frac{N_o}{2}] \mid \hat{C}_k(L) \mid^2$$

The problem is to detect one of M equiprobable, equal energy polyphase signals, and is similar to that described in Section 4-5 of [10]. Hence, the conditional probability $P(e \mid I_L^m)$ can be obtained from the derivation of Section 4-5 replacing the corresponding decision variables by $\{u_1(L) \mid I_L^m, \theta_i(L)\}$ and $\{v_1(L) \mid I_L^m, \theta_i(L)\}$. The result is:

$$P(e \mid I_L^m) = \frac{M-1}{M} - \frac{1}{2} \operatorname{erf}\left[\sqrt{\gamma} \sin\frac{\pi}{M}\right]$$

$$- \frac{1}{\sqrt{\pi}} \int_0^{\sqrt{\pi} \sin\frac{\pi}{M}} \exp(-y^2) \operatorname{erf}\left[y \cot\frac{\pi}{M}\right] dy \qquad (3.69)$$

where

$$\gamma = \frac{A^2 E_p \left[\sum_{k=1}^{N_d} \mid \hat{C}_k(L) \mid^2\right]^2}{\sum_{k=1}^{N_d} [A^2 E_p \, 2\sigma_{Lk}^2 + N_o] \mid \hat{C}_k(L) \mid^2} \qquad (3.70)$$

Now using (3.29) in (3.70) yields

$$\gamma = \frac{A^2 E_p}{N_o[1 + \frac{1}{M_b}]} \sum_{k=1}^{N_d} \mid \hat{C}_k(L) \mid^2 = \frac{x_L}{2\sigma_e^2} \qquad (3.71)$$

where

$$x_L = \sum_{k=1}^{N_d} \mid \hat{C}_k(L) \mid^2 \quad \text{and} \quad 2\sigma_e^2 = \frac{N_o}{A^2 E_p} [1 + \frac{1}{M_b}]$$

Now, from (3.69) and (3.71) the average probability of error can be written as:

$$P(e) = \int_0^\infty P(e \mid I_L^m)\, P(x_L)\, dx_L$$

$$= \int_0^\infty P(e \mid x_L)\, P(x_L)\, dx_L \qquad (3.72)$$

For a uniform delay power profile $P(x_L)$ is given by (3.61). Substituting (3.61) and (3.69) in (3.72) and integrating yields:

$$P(e) = \frac{M-2}{M} + \frac{1}{2}\left[1 - \mu_1 \sum_{k=0}^{N_d-1} \binom{2k}{k} \left(\frac{1-\mu_1^2}{4}\right)^k\right]$$

$$- \frac{1}{\sqrt{\pi}} \sum_{k=0}^{N_d-1} \left(\frac{1-\mu_1^2}{\mu_1^2}\right)^k \frac{1}{k!} \cdot I(k, \mu_1, M) \qquad (3.73)$$

where

$$I(k, \mu_1, M) = \int_0^\infty y^{2k} \exp\left(-\frac{y^2}{\mu_1^2}\right) \operatorname{erf}\left(y \cot\left(\frac{\pi}{M}\right)\right) dy$$

and

$$\mu_1 = \left[\frac{\sin^2\left(\frac{\pi}{M}\right) 2\lambda_L^2}{\sin^2\left(\frac{\pi}{M}\right) 2\lambda_L^2 + 2\sigma_e^2}\right], \quad 2\lambda_L^2 = 2\lambda_{Lk}^2 = \frac{1}{N_c} - 2\sigma_{Lk}^2$$

From (3.73) it is observed that for M=2 (BPSK) a closed form expression is obtained and is given by:

<u>BPSK</u>

$$P(e) = \frac{1}{2}\left[1 - \mu_1 \sum_{k=0}^{N_d-1} \binom{2k}{k} \left(\frac{1-\mu_1^2}{4}\right)^k\right] \qquad (3.74)$$

where

$$\mu_1 = \frac{A^2 E_p \, 2\lambda_L^2}{A^2 E_p \, 2\lambda_L^2 + N_o[1 + \frac{1}{M_b}]}$$

For $M > 2$ the probability of error evaluation requires one numerical integration due to $I(k, \mu_1, M)$.

3.8.2 Non-Uniform Delay Power Profile

This case corresponds to dissimilar paths and hence the average SNR on each path differs. The probability of error is expressed as in (3.72), where $P(x_L)$ is given in (3.46). Hence, using (3.46) and (3.69) in (3.72) and solving the integral yields:

$$P(e) = \frac{M-1}{M} - \sum_{k=1}^{N_d} \pi_{Lk} \, \mu_k \left\{ 1 - \frac{1}{\pi} \tan^{-1} \left[\frac{\tan(\frac{\pi}{M})}{\mu_k} \right] \right\} \qquad (3.75)$$

where

$$\mu_k = \left[\frac{\sin^2 \frac{\pi}{M} \, 2\lambda_{Lk}^2}{\sin^2 \frac{\pi}{M} \, 2\lambda_{Lk}^2 + 2\sigma_e^2} \right]^{\frac{1}{2}}$$

and

$$2\sigma_e^2 = \frac{N_o}{A^2 E_p} \left[1 + \frac{1}{M_b} \right]$$

Now, from (3.75) for $M=2$ (BPSK) the probability of error is given by:

$$P(e) = \frac{1}{2} \left[1 - \sum_{k=1}^{N_d} \pi_{Lk} \left\{ \frac{A^2 E_p \, 2\lambda_{Lk}^2}{A^2 E_p \, 2\lambda_{Lk}^2 + N_o[1 + \frac{1}{M_b}]} \right\}^{\frac{1}{2}} \right] \qquad (3.76)$$

3.8.3 Approximations and Bounds

For $M > 2$ it is necessary to perform a numerical integration in order to evaluate the error probability over a channel with a uniform delay power profile. It was determined that by approximating $P(e \mid \mathbf{I}_L^m)$ a very good approximation to the error probability, in closed form, can be obtained.

From [10], (3.69) can be approximated as:

$$P(e \mid \mathbf{I}_L^m) \simeq \text{erfc}\left[\sqrt{\gamma}\sin\frac{\pi}{M}\right] \tag{3.77}$$

Using (3.77) in (3.72) and performing the appropriate integrations, for uniform and non-uniform profiles, the following expressions for probability of bit error are obtained:

Uniform Delay Power Profile

$$P(e) \simeq 1 - \mu_1 \sum_{k=1}^{N_d-1} \binom{2k}{k} \left[\frac{1-\mu_1^2}{4}\right]^k \qquad M > 2 \tag{3.78}$$

where μ_1 is defined as in (3.73)

Non-Uniform Delay Power Profile

$$P(e) \simeq 1 - \sum_{k=1}^{N_d} \pi_{Lk}\,\mu_k \qquad M > 2 \tag{3.79}$$

where μ_k is defined in (3.75) and π_{Lk} is defined in (3.46).

For QPSK (M=4) and Gray encoding of source bits, it is known that the probability of error is given in [10] as:

$$P_{QG}(e) \simeq \frac{P(e)}{\log_2 M} \tag{3.80}$$

Substituting (3.78) for P(e) in (3.80) yields (3.74), indicating that QPSK with Gray encoding of source bits gives the same error

probability as BPSK. QPSK, however, has twice the throughput for the same error rate.

3.8.4 Differential Detection

The probability of error expressions for DPSK and differential detection can be obtained from (3.75) and (3.77) using $M_b = 1$.

It is to be noted that all the probability of error expressions in this section hold only for $2\alpha_{Lk}^2 > 2\sigma_{Lk}^2$, $k = 1, 2, ..., N_d$. This is reasonable since if the reverse were true it would imply that the estimated SNR is negative.

3.9 Performance Evaluation for Polyphase Signaling

The performance is evaluated with regard to observing the effects of delay power profile, diversity order, estimator memory size, R.M.S delay spread and signaling alphabet size on probability of error. The performance of the coherent receiver is also compared with that of a differential, square-law and a partially coherent receiver.

The performance evaluations are conducted for a quasi-static slowly fading Rayleigh channel. An Uniform, an Exponential and an Irregular delay power profile were used in evaluating the error performance. The non-uniform profiles were assumed to have a 250 ns delay spread with a 40 dB dynamic range in signal levels. The Uniform profile was assumed to have a total delay spread of 250 ns. A signaling rate of 32 kbps and a code length of 255 chips was chosen. It is assumed, as before, that perfect bit and chip synchronization exists. The results of the performance are illustrated in Figures 3.12 - 3.19

The following conclusions were drawn from the performance evaluations:

1. The partially coherent receiver has a BER that is bounded on the lower end by the BER of the coherent Rake receiver and on the upper end by the BER of a Square-Law Rake receiver.
2. When the fade rate is larger than the bandwidth of the estimator filter, decorrelated estimates occur and the BER performance of the partially coherent receiver approaches the upper bound.
3. DDE produces a lower BER than NDDE due to a 3 dB gain in phase estimation SNR, under the ideal assumption that no bit decision errors are made. To prevent propagation of bit errors in memory, it is suggested that short memory lengths ($M_b \leq 10$) or exponential weights be employed.
4. The sample mean estimator performs as well as the Wiener-Hopf estimator when its memory length is chosen by (3.59).

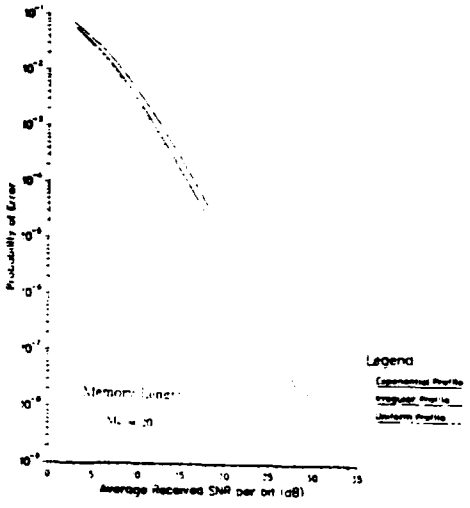

Figure 3.12 Effect of delay power profile on probability of error for coherent receiver (N_d=3).

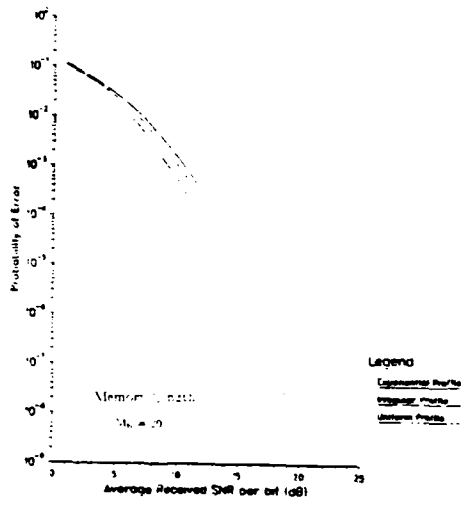

Figure 3.13 Effect of delay power profile on probability of error for coherent receiver (N_d=6).

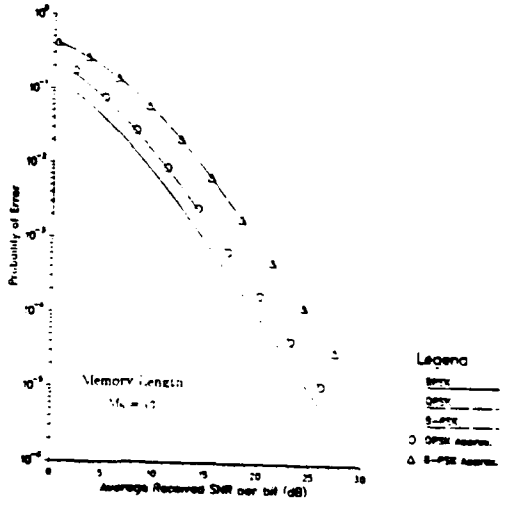

Figure 3.14 Probability of error for polyphase signaling, (N_d=2) - Exponential delay power profile.

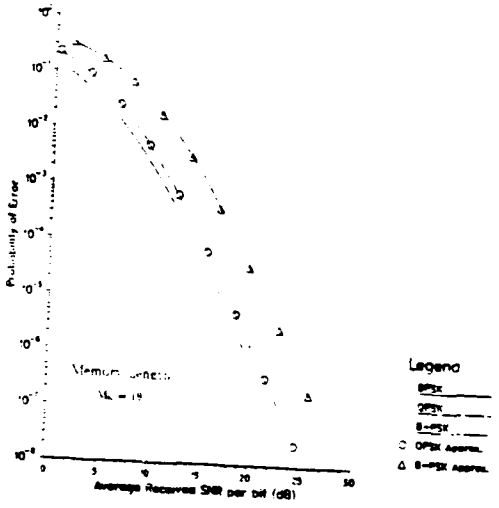

Figure 3.15 Probability of error for polyphase signaling, (N_d=4) - Exponential delay power profile.

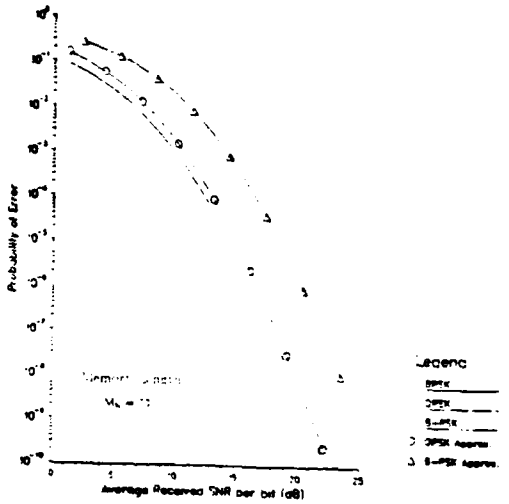

Figure 3.16 Probability of error for polyphase signaling, (N_d=8) - Exponential delay power profile.

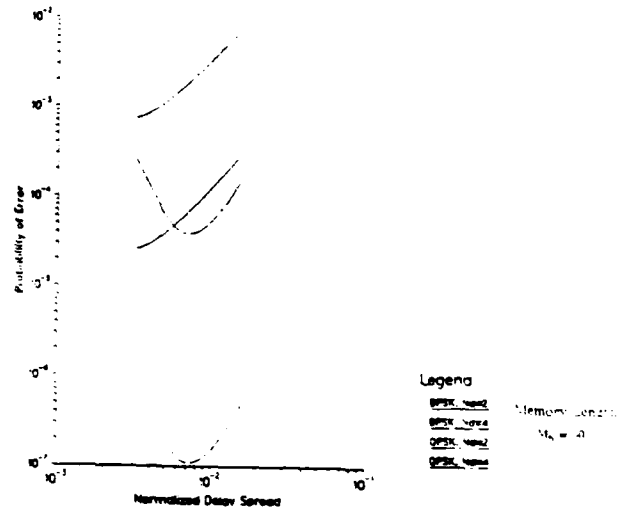

Figure 3.17 Probability of error versus normalized delay spread - Gaussian delay power profile.

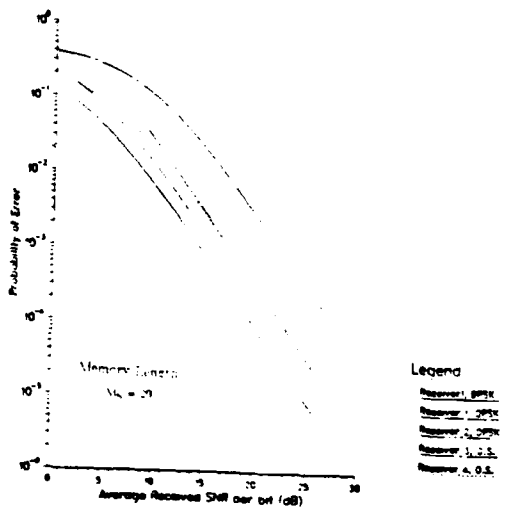

Figure 3.18 Comparison of probability of error for different receivers (N_d=2) - Exponential delay power profile.

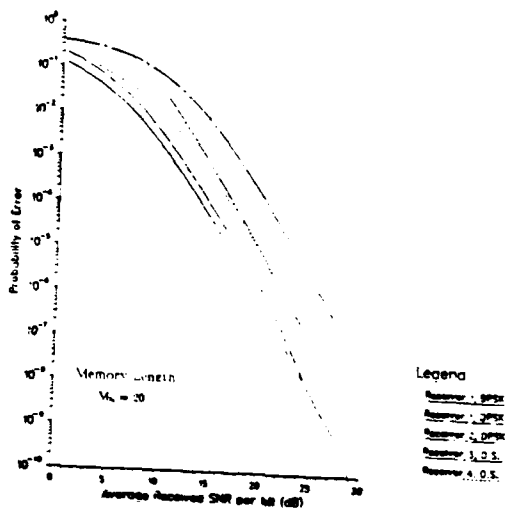

Figure 3.19 Comparison of probability of error for different receivers (N_d=4) - Exponential delay power profile.

5. Large orders of diversity result in inclusion of weak paths and hence large memory lengths (3.59). This results in decorrelated estimates and an increase in BER. Hence, lower orders of diversity are recommended.
6. For a quasi-static channel coherent reception using MRC and DDE is feasible.
7. The coherent receiver like the ONMD receiver is sensitive to the shape of the delay power profile. This emphasizes the need for measuring indoor channel profiles to determine the appropriate transmission power.
8. The coherent receiver is sensitive to R.M.S delay spread variation and exhibits a greater degradation with increasing orders of diversity. This also suggests lower order of diversity. The receiver is more sensitive to delay spread than the shape of the delay power profile.
9. Considerable diversity gain is achieved in using higher orders of diversity. This is offset by the sensitivity to R.M.S delay spread and increase in memory length. An encouraging alternative to achieve higher orders of diversity is to use a low order of multipath diversity and employ multiple antennas.
10. The use of a higher signaling alphabet results in a severe performance degradation for $M > 4$. BPSK and QPSK with Gray encoding or source bit perform equally well. QPSK, however, offers twice the data rate within the same bandwidth.
11. For a quasi-static channel the use of phase coded signaling (BPSK) and MRC results in 3 dB improved performance over differential detection using DPSK signaling.
12. Orthogonal Signaling using partially coherent reception performs as well as DPSK using differential detection. However, the simplicity of the differential detector favors its use in practice.

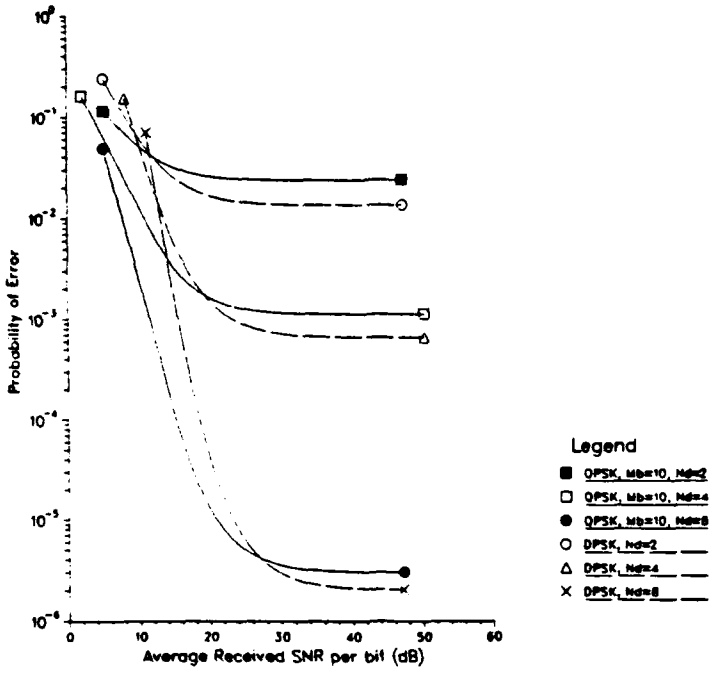

Figure 4.5 Probability of error for QPSK and DPSK in a CDMA system.

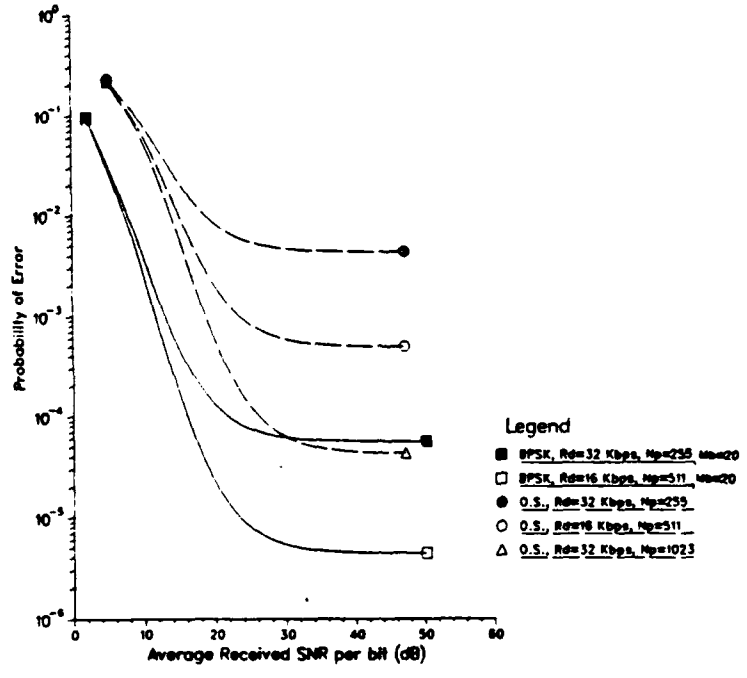

Figure 4.6 Effect of increase in code length on probability of error for Orthogonal Signaling (O.S.) relative to BPSK.

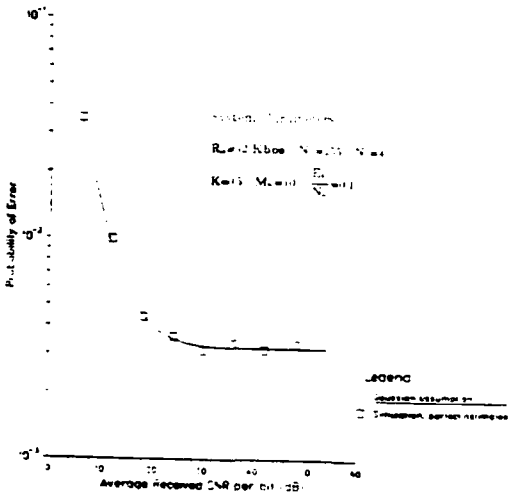

Figure 4.7 Simulation results for probability of error for BPSK considering perfect estimation (N_d=2)

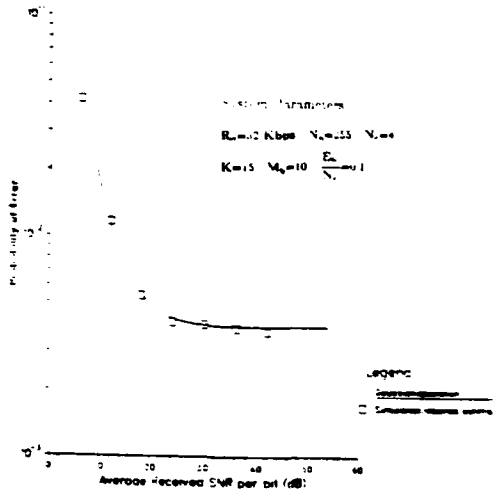

Figure 4.8 Simulation results for probability of error for BPSK considering estimation errors (N_d=2).

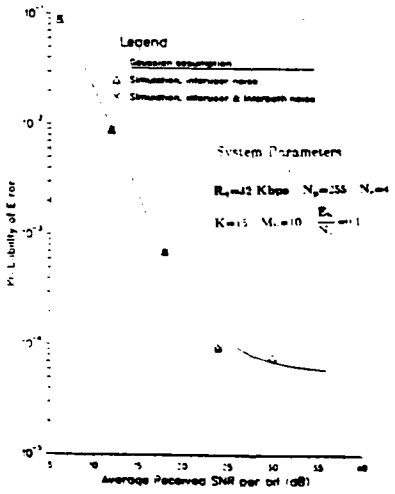

Figure 4.9 Simulation results for probability of error for BPSK considering estimation errors (N_d=4).

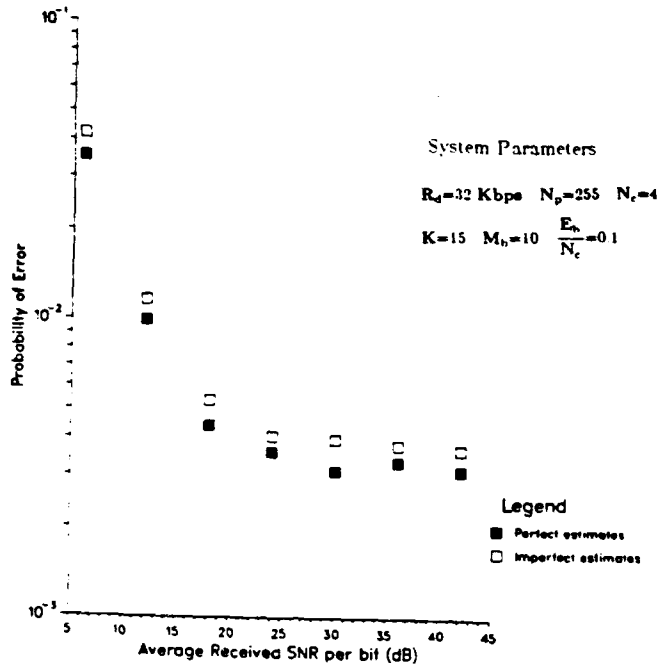

Figure 4.10 Simulation results indicating effect of imperfect estimates.

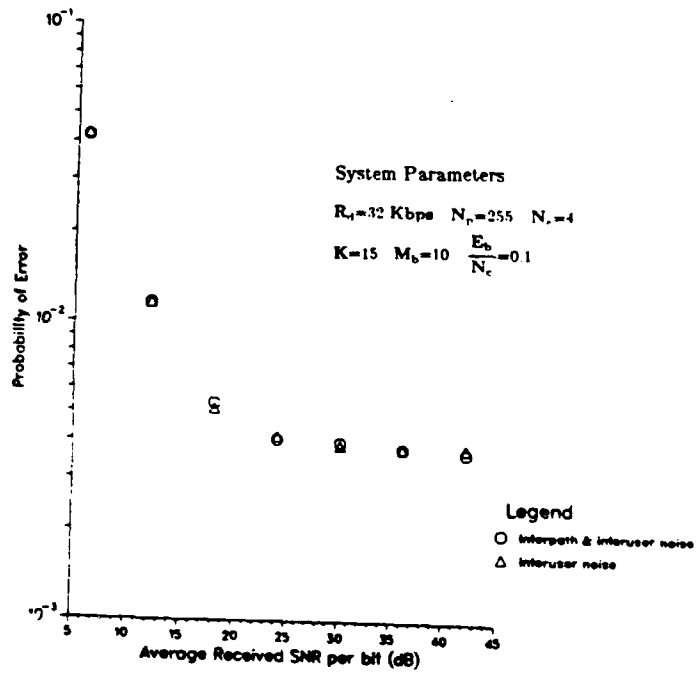

Figure 4.11 Simulation results indicating effect of interpath interference.

CHAPTER 4

COMPARISON OF MULTIPATH DIVERSITY RECEIVERS IN A CDMA SYSTEM

4.1 Introduction

It is the purpose of this chapter to study the performance of three multipath diversity receivers in a multiple-user environment (CDMA) taking into account ISI, interuser interference and non-ideal code correlation effects. In evaluating the probability of error for the different receiver structures, the following CDMA system is considered. The channel is an indoor wireless communication channel. Each user can transmit speech at a rate of 32 kbps. Data will be transmitted in packets. It is assumed that the user terminals communicate with the base station in a star network architecture, [7], [8]. The users communicate to the base station using asynchronous CDMA.

The central station is assumed to have a bank of receivers, one for each unique user code. These receivers are multipath diversity receivers. Each user terminal has a similar receiver structure. To avoid the near-far problem average power control is assumed.

4.2 Performance Analysis

4.2.1 Coherent Multipath Diversity Receiver

Considering BPSK the band-pass transmitted signal for the k^{th} user in the CDMA system is represented as:

$$s_k(t) = \mathrm{Re}[A\ u_k(t)\ e^{j2\pi f_c t}] \tag{4.1}$$

where f_c is the carrier frequency, A is the signal amplitude and

$$u_k(t) = b_k(t)\ p_k(t) \tag{4.2}$$

where $b_k(t)$ is the data bit stream of the k^{th} user and $p_k(t)$ is the corresponding DSSS code.

$$b_k(t) = \sum_{i=-\infty}^{\infty} b_i^k\ g_T(t - iT) \quad ; \quad \{b_i^k\} = \pm 1 \tag{4.3}$$

$$p_k(t) = \sum_{j=-\infty}^{\infty} p_k[j]\, g_{T_p}(t - iT_p) \quad ; \quad \{p_k[j]\} = \pm 1 \tag{4.4}$$

where $g_\tau(t) = 1 \quad 0 \le t \le \tau$ and zero otherwise. It is assumed that the DSSS codes are periodic with period N_p and that $T = T_p\, N_p$. The energy in each period of the code sequence is denoted by E_p.

Consider K asynchronous users of the communication channel. Assuming the channel model of [12] the received signal in the interval, $(L-1)T \le t \le LT$, can be written as:

$$r(t) = \sum_{k=1}^{K} \sum_{m=1}^{N_c} A\, C_m^k(L)\, u_k(t - t_k - mT_p) + \eta(t) \tag{4.5}$$

where $\eta(t)$ is an additive white zero mean complex Gaussian noise process, at the receiver input, with autocorrelation function $\phi_n(t, \tau) = N_o\, \delta(t - \tau)$. t_k is a uniform random variable, in $[0, T - T_m]$, representing the time of transmission for each user. It is assumed that k=1 corresponds to the reference user and that $t_1 = 0$. $C_m^k(L)$ is the m^{th} channel coefficient for the k^{th} user in the interval $(L-1)T \le t \le LT$. The $C_m^k(L)$ are uncorrelated, zero mean complex Gaussian random variables with variance

$$E[\,|C_m^k(L)|^2] = 2\alpha_{km}^2(L) = T_p\, \Phi_c^k(mT_p;0) \tag{4.6}$$

where, $\Phi_c^k(\tau;t)$ is the channel delay power profile for the k^{th} user.

The receiver structure is given by (3.66) and can be rewritten for the reference user (k=1) as:

$$\sum_{j=1}^{N_d} \mathrm{Re}[r_j^1(L)\, \hat{C}_j^{1*}(L)] \underset{H(L) = H_0}{\overset{H(L) = H_1}{\gtrless}} 0 \tag{4.7}$$

where

$$r_m^1(L) = \int_{(L-1)T}^{LT} r(t)\, \frac{1}{\sqrt{E_p}}\, p_1(t_1 - m\, T_p)\, dt \quad ; \quad t_1 = t - (L-1)T \tag{4.8}$$

and $\hat{C}_m^1(L)$ is the MMSE estimate obtained as follows:

$$\hat{C}_m^1(L) = \frac{1}{A\sqrt{E_p}\, M_b} \sum_{j=L-M_b}^{L-1} \hat{b}_j^1\, r_m^1(j) \tag{4.9}$$

where $\hat{b}_j$ is the bit decision in the j^{th} signaling interval for the reference user.

Substituting (4.5) in (4.8) and recalling that the codes are periodic, the output of the correlator on j^{th} branch of the receiver can be written as:

$$r_j^1(L) = \frac{A}{\sqrt{E_p}} \sum_{m=1}^{N_d} \int_0^T C_m^1(L)\, p_1(t - \tau_{m1})\, b_1(t - \tau_{m1})\, p_1(t - j\, T_p)\, dt$$

$$+ \frac{A}{\sqrt{E_p}} \sum_{k=2}^{K} \sum_{m=1}^{N_d} \int_0^T C_m^k(L)\, p_k(t - \tau_{mk})\, b_k(t - \tau_{mk})\, p_1(t - jT_p)\, dt$$

$$+ \frac{1}{\sqrt{E_p}} \int_{(L-1)T}^{LT} \eta(t)\, p_1(t_1 - j\, T_p)\, dt \tag{4.10}$$

where $\tau_{mk} = t_k + mT_p$ which is a uniform random variable in the interval [0,T]. Recall $\tau_{m1} = mT_p$. Substituting (4.3) in (4.10) and using the method outlined in [20], [6] (4.10) can be expressed as:

$$r_j^1(L) = A\sqrt{E_p}\, b_L^1\, C_j^1(L) + X_j(L) + Y_j(L) + \eta_j^1(L) \tag{4.11}$$

where

$$X_j(L) = \frac{A}{\sqrt{E_p}} \sum_{\substack{m=1 \\ m \neq j}}^{N_d} C_m^1(L)[b_L^1\, \hat{R}_{11}(\tau_{mj}^1) + b_{L-1}^1\, R_{11}(\tau_{mj}^1)]$$

$$Y_j(L) = \frac{A}{\sqrt{E_p}} \sum_{\substack{m=1 \\ m \neq j}}^{N_d} C_m^k(L)[b_L^1\, \hat{R}_{k1}(\tau_{mj}^k) + b_{L-1}^1\, R_{k1}(\tau_{mj}^k)]$$

$$\hat{R}_{k1}(\tau) = \int_\tau^T p_1(t)\, p_k(t - \tau)\, dt \quad k = 1, 2, \cdots K$$

$$R_{k1}(\tau) = \int_0^T p_1(t)\, p_k(t-\tau)\, dt \quad k = 1, 2, \cdots K$$

$$\tau_{mj}^{k} = t_k + mT_p - j\,T_p \quad ; \quad k = 1, 2, \cdots K \; ; \; t_1 = 0$$

where $\hat{R}_{k1}(\tau)$ and $R_{k1}(\tau)$ are continuous partial correlation functions.

Let $Z_j(L) = X_j(L) + Y_j(L) + \eta_{jL}^1$ represent the total interference on the j^{th} branch of the reference user. $X_j(L)$ represents the interpath interference arising due to the non-ideal autocorrelation of the DSSS codes. $Y_j(L)$ represents the interuser interference arising due to the non-ideal cross-correlation of the DSSS codes.

Substituting (4.11) in (4.7) the basic decision variable becomes:

$$u_1(L) = \sum_{j=1}^{N_d} \mathrm{Re}\left\{\left[A\sqrt{E_p}\, b_L^1\, C_j^1(L) + Z_j(L)\right]\hat{C}_j^{1*}(L)\right\} \tag{4.12}$$

The following assumptions are now made

(i) The delay power profile is uniform.

(ii) $X_j(L)$ is small in comparison to $Y_j(L)$. This is particularly true for low orders of diversity and a large number of active users.

(iii) $Z_j(L) = V_j(L) + \eta_{jL}^1$, is a Gaussian random variable. This is a logical assumption based on the central limit theorem. It can also be shown that $Z_j(L)$ is zero mean and has a variance σ_0^2, which is computed below.

(iv) $\mathbf{E}[Z_j(i)\, Z_j^*(k)] = 0$ when $i \neq k$.

(v) $\mathbf{E}[Z_j(i)\, Z_m^*(i)] = 0$ when $j \neq m$.

Under these assumptions the decision variable given by (4.12) is similar to that given by (3.68a). Hence, the corresponding probability of error will be the same, except that N_o is replaced by σ_o^2 which is the variance of the new noise variable $Z_j(L)$.

Assuming that the interpath interference is much smaller than the interuser interferene, it can be shown that:

$$\sigma_o^2 = E_b \frac{2}{3N_p} \sum_{k=2}^{K} \sum_{m=1}^{N_d} 2\alpha_{km}^2(L) + N_o \tag{4.13}$$

where $E_b = A^2T$ is the transmitted energy per symbol period. For a uniform profile, $2\alpha_{km}^2(L) = \frac{1}{N_c}$, $m = 1, 2, ..., N_c$ and

$$\sigma_o^2 = \frac{E_b}{N_c} \frac{2}{3N_p} N_d(K-1) + N_o \tag{4.14}$$

Hence, for a non-uniform delay power profile, the probability of error is given by (3.77) with N_o replaced by σ_o^2, which is defined in (4.13). For a uniform delay power profile the probability of error is given by (3.75) with N_c replaced by σ_o^2, which is defined in (4.14). For $M > 2$, the probability of error expressions given by (3.73) and (3.76) can be used, appropriately, with N_c replaced by σ_o^2.

4.2.2 Differential Multipath Diversity Receiver

The receiver structure for the k^{th} user may be expressed as:

$$\sum_{m=1}^{N_d} \mathrm{Re}[r_m^k(L)\, r_m^{k*}(L-1)] \underset{H(L)=H_o}{\overset{H(L)=H_1}{\gtrless}} 0 \tag{4.15}$$

This receiver structure can be obtained from (4.7) and (4.9) using $M_b = 1$. Hence, the probability of error for the differential receiver can be obtained from the probability of error expressions of the coherent receiver by using $M = 2$ and $M_b = 1$.

4.2.3 Non-Coherent Multipath Diversity Receiver

Each user employs a pair of orthogonal codes to transmit binary information. Let $p_{k1}(t)$ and $p_{k0}(t)$ denote the pair of codes used by the k^{th} user. The received signal can be represented as:

$$r(t) = \sum_{k=1}^{K} \sum_{m=1}^{N_d} A\, C_m^k(L) \left[\sum_{i=-\infty}^{\infty} a_i^k\, g_T(t - \tau_{mk} - iT)\, p_{k1}(t - \tau_{mk}) \right.$$

$$\left. + (1 - a_i^k)\, g_T(t - \tau_{mk} - iT)\, p_{ko}(t - \tau_{mk}) \right] + \eta(t) \tag{4.16}$$

where

$$p_{ki} = \sum_{j=-\infty}^{\infty} p_{ki}[j]\, g_{T_p}(t - j\,T_p) \;\; ; \;\; \{p_{ki}[j]\} = \pm 1 \;\; ; \;\; i = 0, 1 \qquad (4.17)$$

$g_\tau(t) = 1 \quad 0 \le t \le \tau$ and zero otherwise. A is the signal amplitude. a_i^k indicates which hypothesis is true in the i^{th} signaling interval. a_i^k=0 when H(i)=H_0 and a_i^k=1 when H(i)=H_1. t_k is a uniform random variable, in $[0, T-T_m]$, representing the random time of transmission of each of the K asynchronous users. $\eta(t)$ is a zero mean complex Gaussian random process with autocorrelation function $N_o\,\delta(t-\tau)$.

Assuming a uniform delay power profile, the receiver structure for the k^{th} user is expressed as:

$$\sum_{m=1}^{N_d} |r_k^1(L)|^2 \underset{H(L)=H_0}{\overset{H(L)=H_1}{\gtrless}} \sum_{m=1}^{N_d} |r_{km}^{\circ}(L)|^2 \qquad (4.18)$$

where

$$r_{km}^{1}(L) = \int_{(L-1)T}^{LT} r(t)\, p_{ki}(t_1 - mT_p)\, dt \quad ; \quad i = 0, 1 \qquad (4.19)$$

and $t_1 = t - (L-1)T$

Assume that in the L^{th} signaling interval, the reference user transmits $p_{11}(t)$. Now, substituting (4.16) in (4.19) it can be shown that the output of the j^{th} branch correlator of the reference user's receiver is:

$$r_{1j}^1(L) = A\sqrt{E_p}\, C_j^1(L) + X_{1j}(L) + Y_{1j}(L) + \eta_{1j}^1(L) \qquad (4.20)$$

$$r_{1j}^{\circ}(L) = A\sqrt{E_p} \left(\frac{\theta_{10}^1(0)}{E_p}\right) C_j^1(L) + X_{oj}(L) + Y_{oj}(L) + \eta_{oj}^1(L) \qquad (4.21)$$

where, for i = 0, 1

$$X_{ij}(L) = \frac{A}{\sqrt{E_p}} \sum_{\substack{m=1 \\ m \neq j}}^{N_d} C_j^1(L) \left[a_L^1\, \hat{R}_{11}^{11}(\tau_{mj}^1) + (1 - a_L^1)\, \hat{R}_{01}^{11}(\tau_{mj}^1)\right.$$

$$+ a_{L-1}^{1} R_{1i}(\tau_{mj}^{1}) + (1 - a_{L-1}^{1}) R_{oi}(\tau_{mj}^{1})$$

$$Y_{ij}(L) = \frac{A}{\sqrt{E_p}} \sum_{k=2}^{K} \sum_{m=1}^{N_d} C_j^k(L) \left[a_L^k \hat{R}_{1i}^{k1}(\tau_{mj}^{k}) + (1 - a_L^k) \hat{R}_{oi}^{k1}(\tau_{mj}^{1}) \right.$$

$$\left. + a_{L-1}^{k} R_{1i}^{k1}(\tau_{mj}^{k}) + (1 - a_{L-1}^{k}) R_{oi}^{k1}(\tau_{mj}^{k}) \right]$$

$$\hat{R}_{li}^{k1}(\tau) = \int_{\tau}^{T} p_{kl}(t-\tau)\, p_{1i}(t)\, dt \quad ; \quad l = 0, 1$$

$$R_{li}^{k1}(\tau) = \int_{0}^{\tau} p_{kl}(t-\tau)\, p_{1i}(t)\, dt \quad ; \quad l = 0, 1$$

$$\tau_{mj}^{k} = t_k + mT_p - jT_p \quad ; \quad k = 1, 2, \cdots K \; ; \; t_1 = 0$$

$$\eta_{ij}^{1}(L) = \frac{1}{\sqrt{E_p}} \int_{(L-1)T}^{LT} \eta(t)\, p_{1i}(t_1 - jT_p)\, dt$$

$$\theta_{10}^{1}(0) = \sum_{j=0}^{N_p-1} p_{11}[j]\, p_{10}[j]$$

$\theta_{10}^{1}(0)$ is the periodic cross-correlation of the DSSS codes. Also, $a_i^k = 1$ if $p_{k1}(t)$ is sent in the i^{th} signaling interval and $a_i^k = 0$ if $p_{k0}(t)$ is sent in the i^{th} signaling interval; the choice determined as a Bernoulli event. $\hat{R}_{li}^{k1}(\tau)$ and $R_{li}^{k1}(\tau)$ are continuous-time partial correlation functions

$\eta_{ij}^{1}(L)$, $i = 0, 1$ represent two zero mean complex Gaussian random variables with variance N_o. The correlation between these noise variables can be shown to be:

$$E[\eta_{j1}^{1}(L)\,\eta_{jo}^{1}{}^{*}(L)] = N_o \left[\frac{\theta_{10}^{1}(0)}{N_p}\right] \qquad (4.22)$$

For each receiver the total interference in the two arms (i = 0, 1) are defined as:

$$Z_{ij}(L) = X_{ij}(L) + Y_{ij}(L) + \eta_{ij}^{1}(L) \quad , \quad i = 0, 1 \qquad (4.23)$$

where $X_{ij}(L)$ is the interpath interference, $Y_{ij}(L)$ is the interuser interference and $\eta_{ij}^{1}(L)$ is the AWGN interference.

Now, as in Section 4.2.1 the following assumptions are made:

(i) The delay power profile is uniform.

(ii) The interpath interference is negligible in comparison to the interuser interference.

(iii) $Z_{ij}(L) = X_{ij}(L) + \eta_{ij}^{1}(L)$ is modeled as zero mean complex Gaussian noise, with variance σ_i^2, from the central limit theorem.

(iv) $E[Z_{ij}(L)\, Z_{ij}{}^{*}(k)] = 0$ when $L \neq k$

(v) $E[Z_{im}(k)\, Z_{in}{}^{*}(k)] = 0$ when $m \neq n$

(vi) $\dfrac{\theta_{10}^{1}(0)}{N_p} \ll 1$

Using the above assumptions it can be shown that $r_{1j}^{1}(L)$ and $r_{1j}^{0}(L)$ are zero mean correlated complex Gaussian random variables with variances σ_1^2 and σ_0^2. The variance of each of these random variables can be shown to be:

$$\sigma_1^2 = \frac{E_b}{N_c}\left[1 + N_d(K-1)\,\frac{2}{3N_p}\right] + N_o \qquad (4.24)$$

$$\sigma_0^2 = \frac{E_b}{N_c}\left[\frac{\{\theta_{10}^{1}(0)\}^2}{E_p^2} + N_d(K-1)\,\frac{2}{3N_p}\right] + N_o \qquad (4.25)$$

where $E_b = A^2T$ is the transmitted energy per symbol period.

Further, it can be shown that the correlation between the variables $r^1_{km}(L)$ and $r^\circ_{km}(L)$ is given by:

$$\mu^1_{10} = \mathbf{E}[r^1_{km}(L)\ r^\circ_{km}{}^*(L)]$$

$$= \frac{E_b}{N_c}\ N_d(K-1)\ \frac{2}{3N_p}\ \left[\frac{\theta^1_{10}(0)}{N_p}\right] \tag{4.26}$$

To compute the probability of error, the decision variable from (4.18) is expressed as:

$$\Gamma = \sum_{j=1}^{N_d} \left[\ |r^1_{1j}(L)|^2 - |r^0_{1j}(L)|^2\ \right] \tag{4.27}$$

and the probability of error is given by:

$$P(e) = P(\Gamma < 0) \tag{4.28}$$

Using equation (4.21) of [18] and making appropriate changes based on the statistics of $r^1_{mk}(L)$ and $r^\circ_{mk}(L)$ it can be shown that:

$$P(e) = \frac{1}{\left[1 + \frac{V_2}{V_1}\right]^{2N_d-1}} \sum_{m=0}^{N_d-1} \binom{2N_d-1}{m} \left(\frac{V_2}{V_1}\right)^m \tag{4.29}$$

where,

$$u = \sigma_1^2\ \sigma_0^2 - |\mu^1_{10}|^2$$

$$W = \frac{\sigma_1^2 - \sigma_0^2}{2u}$$

$$V_1 = (W^2 + \frac{1}{u})^{1/2} - W$$

$$V_2 = (W^2 + \frac{1}{u})^{1/2} + W$$

4.3 Receiver Performance Comparison

In this section a comparison is made of the BER performance of three receivers, under the following conditions: uniform delay power profile with $T_m = 400$ ns, $R_d = 32$ kbps, $N_p = 255$, $E_b/N_c = -10$ dB, $K = 15$, $N_c = 4$ and $M_b = 10$.

Figure 4.1 illustrates the effect of a non-ideal cross-correlation for Gold codes used in binary orthogonal signaling. It is seen that the code cross-correlation raises the irreducible BER due to a correlation between the diversity branches. Figure 4.2 illustrates that for Kasami codes the degradation from ideal performance is small. This is because these Kasami codes are optimal [18], as they satisfy Welch's lower bound for the peak cross-correlation value.

Figure 4.3-4.5 illustrate a comparison of three modulation and detection schemes. It is observed that interuser interference produces an irreducible BER or error floor. From the error floors it can be seen that BPSK-coherent detection offers almost a 3dB advantage over DPSK-differential detection. DPSK-differential detection offers almost a 4 dB advantage over orthogonal signaling (O.S.)- non-coherent detection. It is also seen that for higher orders of diversity, $N_d = 8$, there is a significant performance improvement. Since $N_c = 4$, this order of diversity can be achieved through antenna diversity by employing two antennas. Figure 4.5 illustrates an interesting result, where it is seen that DPSK-differential detection produces a lower irreducible BER than QPSK-coherent detection, indicating that DPSK-differential detection performs better when the interuser interference becomes the limiting noise source.

Non-coherent detection, although simple to implement, offers very poor performance. To obtain better performance, for a given order of diversity, there are two alternatives. The first is to use a longer DSSS code, results for which are shown in Figure 4.6. It is seen that in order to obtain a performance on the order of BPSK-coherent detection, it is necessary to use a code that is four times as long. However, if this performance improvement is to be achieved for the same order of diversity the data rate must be divided by 4. In other words, for a given bandwidth and delay spread, a performance gain can be achieved using a longer code but the data rate must be appropriately reduced.

4.4 Simulation Study

In evaluating the performance of the receivers for a multi-user system a number of assumptions were made for tractable analysis. These assumptions could result in highly biased results.

In practice, the interpath interference and the interuser interference produce some correlation between the diversity branches which

negates the effect of diversity combining, [2], [9]. Further, the effect of the total interference may be such that the simple sample mean estimator may not be adequate for coherent detection.

In order to observe the severity of these effects and verify the earlier assumptions a small CDMA system was simulated. The simulation study was conducted for a 15 user system using 255 chip long Kasami sequences. For this system the following parameters were assumed:

(i) A uniform delay power profile with a multipath spread of 400 ns. This allows a maximum diversity order of $N_d = 4$ for Kasami codes of length 255 chips and a data rate of 32 kbps.

(ii) Average power control is assumed.

(iii) Each user employs BPSK signaling at 32 kbps and coherent detection using MRC.

(iv) The sample mean estimator of (4.40) with $M_b = 10$ was used in all receivers. Since the probability of error of interest is around 10^{-4} the effect of bit decision errors on DDE were neglected.

(v) The Kasami sequences used are Auto-Optimal Least Side Lobe Energy (AO/LSE) sequences, [21]. AO/LSE codes produce very low-interference when used in CDMA applications. These codes were generated using the initial loadings given in [21].

The Monte Carlo technique was used to simulate the system. A sample size of 10^{k+2} was used to estimate error probabilities of the order 10^{-k}. From [3], it can be shown that this sample size produces a 99% confidence interval of [1.29 P(e), 0.77 P(e)]; where P(e) denotes the estimated error probability.

The results of the simulation are presented in Figures 4.7-4.11. The simulation runs resulted in a normalized error of less than 11%. The normalized error variance was computed to be less than 0.03%. Based on the limited simulation results the following conclusions are made:

(i) The interuser interference can be modeled as additive Gaussian noise when the product of the number of active users and resolved paths is large.

(ii) The interpath interference is small in comparison to the interuser interference for small delay spreads. Hence, it can be neglected in order to simplify the analysis.

(iii) The sample mean estimator performs adequately in the presence of interuser interference.

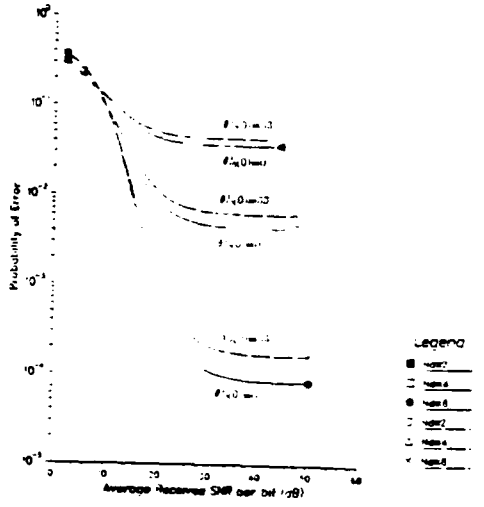

Figure 4.1 Bounds on irreducible error for Orthogonal Signaling (O.S.) using Gold codes.

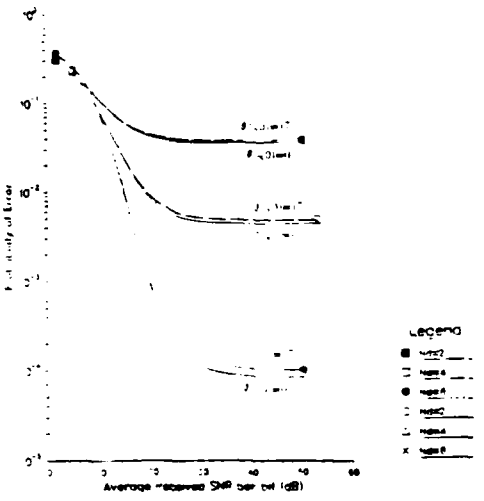

Figure 4.2 Bounds on irreducible error for Orthogonal SIgnaling (O.S.) using Kasami codes.

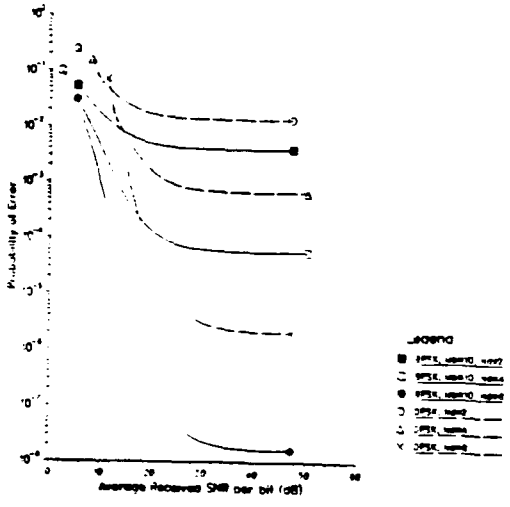

Figure 4.3 Probability of error for BPSK and DPSK in a CDMA system.

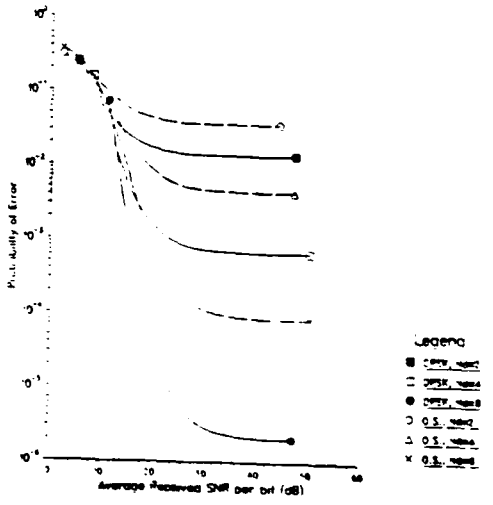

Figure 4.4 Probability of error for DPSK and Orthogonal signaling (O.S.) in a CDMA system.

4.5 Conclusions

Three multipath diversity receivers using coherent, differential and non-coherent detection, respectively, were analyzed based on the assumptions that there is average power control and interuser interference is Gaussian. The performance results indicated that BPSK using coherent detection performs the best, followed by DPSK using differential detection. The use of orthogonal signaling and non-coherent detection requires the use of long codes, which in turn stipulates lower data rates for a given bandwidth and delay spread. It is seen that antenna diversity in conjunction with low orders of multipath diversity produce significant BER performance gain. The simplifying assumptions involved in the performance analysis were verified through simulation.

REFERENCES

[1] Candy, J.V, *Signal Processing - The Model Based Approach*, McGraw Hill, Singapore, 1986.

[2] Jakes, W.C, *Microwave Mobile Communication*, John Wiley and Sons, New York, 1974.

[3] Jeruchim, M.C, "Techniques for Estimating the Bit Error Rate in the Simulation of Digital Communication Systems", IEEE Journal on Selected Areas in Comm., Vol. SAC-2, No. 1, pp. 153-170, January 1984.

[4] Kam, P.Y, and C.H.Teh, "An Adaptive Receiver with Memory for Slowly Fading Channels", IEEE Trans. on Comm. Theory, Vol. COM-32, No.6, pp. 654-659, June 1984.

[5] Kam, P.Y, and C.H. Teh, "Adaptive Diversity Reception over a Slow Non-Selective Fading Channel", IEEE Trans. on Comm., Vol. COM-35, No. 5, pp. 572-574, May 1987.

[6] and Diversity for Spread Spectrum in Indoor Wireless Communication", AT&T Tech. Journal, Vol. 64, pp. 1927-1965, October 1985.

[7] Kavehrad, M, and B. Ramamurthi, "Direct Sequence Spread Spectrum with DPSK Modulation and Diversity for Indoor Wireless Communications", IEEE Trans. on Comm., Vol. COM-35, No. 2, pp. 224-236, February 1987.

[8] Kavehrad, M, and P.J. McLane, "Spread Spectrum for Indoor Digital Radio", IEEE Comm. Magazine, Vol. 25, No. 6, pp. 32-40, June 1987.

[9] Lee, W.C.Y, *Mobile Communications Engineering*, McGraw Hill, 1982.

[10] Lindsey, W.C, and M.K. Simon, *Telecommunications Systems Engineering*, Chapter 5, Prentice Hall, 1973.

[11] Musser, J.M, and J.N. Daigle, "Throughput Analysis of an Asynchronous Code Division Multiple Access (CDMA) System", Proc. of ICC, 2.F.2.1-2.F.2.7, 1982.

[12] Ochsner, H, "Direct Sequence Spread Spectrum Receiver for Communication on Frequency Selective Fading Channels", IEEE Journal on Selected Areas in Comm., Vol. SAC-5, No. 2, pp. 188-193, February 1987.

[13] Pahlavan, K, "Wireless Communications for Office Information Networks", IEEE Comm. Magazine, Vol. 23, N0.6, pp. 19-27, June 1985.

[14] Papoulis, A, *Probability, Random Variables and Stochastic Processes*, Second Edition, McGraw Hill, 1984.

[15] Parl, S, "A New Method of Calculating Generalized Q-Functions", IEEE Trans. Info. Theory, Vol. IT-26, No.1, pp. 121-124, January 1980.

[16] Price, R, and P.E. Green, "A Communication Technique for Multipath Channels", Proc. IRE, Vol. 46, pp. 555-570, March 1958.

[17] Proakis, J.G, P.R. Drouhillet Jr., and R. Price, "Performance of Coherent Detection Systems Using Decision-Directed Channel Measurement", IEEE Trans. on Comm. Systems, pp. 54-63, March 1968.

[18] Proakis, J.G, *Digital Communications*, McGraw Hill, 1983

[19] Proakis, J.G, "Probabilities of Error for Adaptive Reception of M-Phase Signals", IEEE Trans. on Comm. Tech., Vol. COM-16, No.1, pp. 71-81, February 1986.

[20] Pursley, M.B, "Performance Evaluation for Phase Coded Spread Spectrum Multiple Access Communication - Part 1: System Analysis", IEEE Trans. on Comm., Vol. COM-25, No. 8, pp. 795-799, August 1977.

[21] Pursley, M.B, and H.F.A. Roefs, "Numerical Evaluation of Cross-Correlation Parameters for Optimal Phases of Binary Shift Register Sequences", IEEE Trans. on Comm., Vol. COM-27, pp. 1597-1607, October 1979.

[22] Schwartz, M, W.R. Bennett and S. Stein, *Communication Systems and Techniques*, Chapters 9-11, McGraw Hill, 1966.

[23] Van Trees, H.L, Detection, Estimation and Modulation Theory, Part 1, John Wiley and Sons, 1968.

[24] Van Trees, H.L, Detection, Estimation and Modulation Theory, Part 3, Chapters 2-4, John Wiley and Sons, 1971.